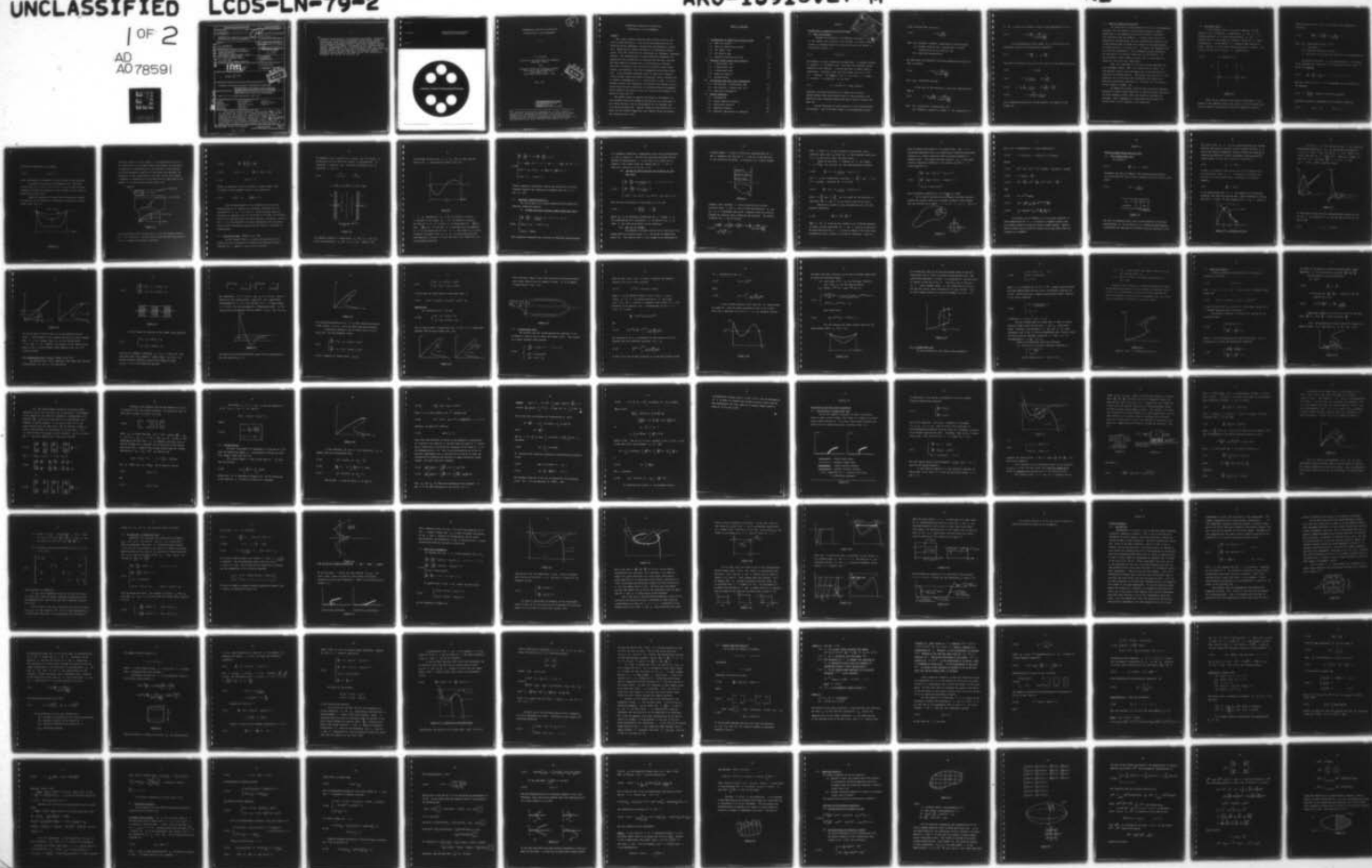


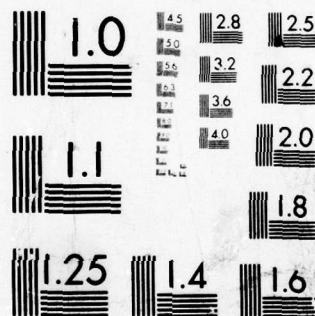
AD-A078 591

BROWN UNIV PROVIDENCE R I LEFSCHETZ CENTER FOR DYNAM--ETC F/G 6/1  
MATHEMATICAL ANALYSIS OF ARTIFICIAL ENZYMATICALLY ACTIVE MEMBRA--ETC(U)  
MAY 79 J P KERNEVEZ DAAG29-76-G-0294  
LCDS-LN-79-2 ARO-13915.27-M NL

UNCLASSIFIED

1 OF 2  
AD  
AD 78591





MICROCOPY RESOLUTION TEST CHART  
NATIONAL BUREAU OF STANDARDS-1963-A



REPORT DOCUMENTATION PAGE		READ INSTRUCTIONS BEFORE COMPLETING FORM
1. REPORT NUMBER (19) 13915.27-M	2. GOVT ACCESSION NO. (18) ARO	3. RECIPIENT'S CATALOG NUMBER (11)
4. TITLE (and Subtitle) (6) MATHEMATICAL ANALYSIS OF ARTIFICIAL ENZYMATICALLY ACTIVE MEMBRANES		5. TYPE OF REPORT & PERIOD COVERED (9) Technical rept.
6. PERFORMING ORG. REPORT NUMBER		7. CONTRACT OR GRANT NUMBER(s) (15) ARO DAAG29-76-G-0294 NSF-MCS 79-05774
8. AUTHOR(s) (10) J.P. KERNEVEZ		9. PROGRAM ELEMENT, PROJECT, TASK AREA & WORK UNIT NUMBERS (12) 145
10. PERFORMING ORGANIZATION NAME AND ADDRESS DIVISION OF APPLIED MATHEMATICS BROWN UNIVERSITY PROVIDENCE, RHODE ISLAND 02912		11. REPORT DATE (11) May 1979
11. CONTROLLING OFFICE NAME AND ADDRESS U.S. ARMY RESEARCH OFFICE P.O. Box 1211 TRIANGLE PARK, NORTH CAROLINA		12. NUMBER OF PAGES 99
12. MONITORING AGENCY NAME & ADDRESS (if different from Controlling Office)		13. SECURITY CLASS. (of this report) UNCLASSIFIED
13. DISTRIBUTION STATEMENT (of this Report) (14) LCDS-LN-79-2		14. DECLASSIFICATION/DOWNGRADING SCHEDULE
14. DISTRIBUTION STATEMENT (of the abstract entered in Block 20, if different from Report) APPROVED FOR PUBLIC RELEASE; DISTRIBUTION UNLIMITED.		
15. SUPPLEMENTARY NOTES LCDS LN 79-2, Brown University, May 1979		
16. KEY WORDS (Continue on reverse side if necessary and identify by block number) <div style="display: flex; justify-content: space-between;"> <div>           enzymes membranes immobilization hysteresis oscillation         </div> <div>           wave propagation wave fronts numerical analysis stability bifurcation         </div> <div>           diffusion pattern formation tubularia         </div> </div>		
17. ABSTRACT (Continue on reverse side if necessary and identify by block number) This report contains material from lectures given in May of 1979 while the author was at Brown University. The systems described in this report are immobilized enzyme membranes, produced and experimentally studied by D. Thomas and his group. (Laboratoire de Technologie Enzymatique, E.R.A. 338, Universite de Technologie de Compiegne, Compiegne, France). The concentrations in these artificial membranes are governed by the interaction of diffusion and reaction, and they may have		

ADA 078591

DNC FILE COPY

DDC  
RECEIVED  
DEC 27 1979

401 834

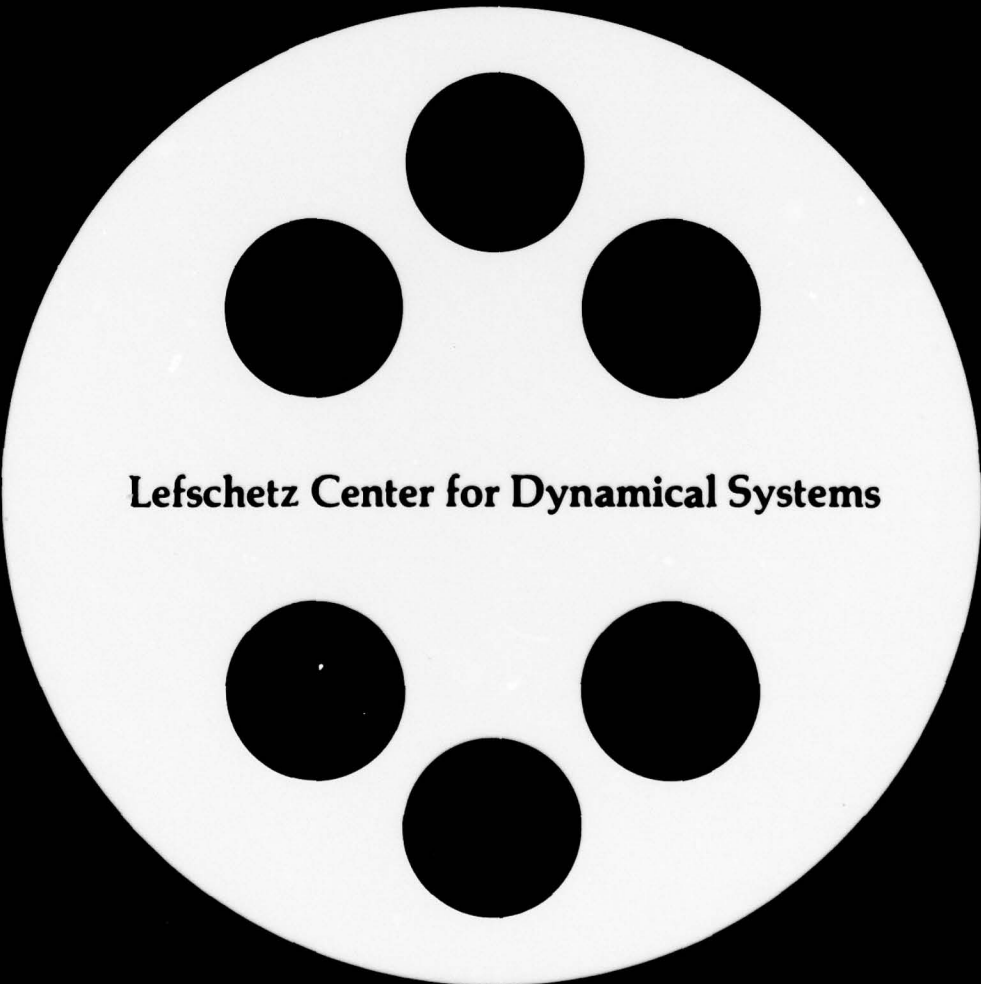
✓ behaviors characteristic of dissipative structures: hysteresis (related to the existence of multiple stable steady states), oscillations, wave front propagation and pattern formation. Since analogous phenomena exist in (much more complex!) living systems (short-term memory, biological clocks, transmission of signals, morphogenesis) it is interesting to study, in a well-defined context, the interaction of diffusion and enzyme reaction. Further details and more references on diffusion-reaction phenomena can be found in the books of Aris [1], Nicolis and Prigogine [2], Murray [3] and Fife [4]. 7

LCDS LN 79-2

J. P. KERNEVEZ

**MATHEMATICAL ANALYSIS OF ARTIFICIAL  
ENZYMATICALLY ACTIVE MEMBRANES**

MAY 1979



**Lefschetz Center for Dynamical Systems**

Division of Applied Mathematics

Brown University Providence RI 02912



(11)

MATHEMATICAL ANALYSIS OF ARTIFICIAL  
ENZYMATICALLY ACTIVE MEMBRANES<sup>†</sup>

by

J. P. Kernevez

University de Technologie de Compiègne  
Compiègne, France

and

Lefschetz Center for Dynamical Systems  
Division of Applied Mathematics  
Brown University  
Providence, Rhode Island 02912

D D C  
DEC 27 1979  
RECEIVED

May, 1979

This document has been approved  
for public release and sale; its  
distribution is unlimited.

---

<sup>†</sup>This research was partially supported by C.N.R.S. (Centre National de la Recherche Scientifique); the production of these lecture notes was supported in part by the National Science Foundation under Contract #NSF-MCS790-174 and in part by the U.S. Army Research Office under Contract #AROD DAAG29-76-G-0294.

# MATHEMATICAL ANALYSIS OF ARTIFICIAL ENZYMATICALLY ACTIVE MEMBRANES

## Preface

This report contains material from lectures given in May 1979 at Brown University. The systems described here are immobilized enzyme membranes, produced and experimentally studied by D. Thomas and his group (Laboratoire de Technologie Enzymatique, E.R.A.338, Université de Technologie de Compiègne, Compiègne, France). The concentrations in these artificial membranes are governed by the interaction of diffusion and reaction, and they may have behaviors characteristic of dissipative structures: hysteresis (related to the existence of multiple stable steady states), oscillations, wave front propagation and pattern formation. Since analogous phenomena exist in (much more complex!) living systems (short-term memory, biological clocks, transmission of signals, morphogenesis) it is interesting to study, in a well-defined context, the interaction of diffusion and enzyme reaction. Further details and more references on diffusion-reaction phenomena can be found in the books of Aris [1], Nicolis and Prigogine [2], Murray [3] and Fife [4].

The author wishes to express his thanks to the members of the Lefschetz Center for Dynamical Systems for its invitation to give these lectures, and to the audience for its patience and its motivating questions. Special thanks are due Professor H. T. Banks for his helpful suggestions and comments while the author was preparing these notes.

## TABLE OF CONTENTS

	page
I. <u>Introduction to immobilized enzyme systems</u>	
1.1. What are enzymes?	1
1.2. What are immobilized enzymes?	4
1.3. The "model" case	5
1.4. The glucose pump	9
1.5. Substrate inhibited kinetics	12
II. <u>Multiple steady states and hysteresis</u>	
2.1. 0-dimensional case	18
2.2. 1-dimensional case	26
2.3. 2-dimensional case	30
2.4. Numerical analysis	33
2.5. Optimum design	37
III. <u>Oscillations and wave front propagation</u>	
3.1. Oscillations: 0-dimensional case	43
3.2. Oscillations: 1-dimensional case	50
3.3. Wave-front propagation	53
IV. <u>Pattern formation</u>	
4.1. Introduction	60
4.2. Linear stability analysis	70
4.3. Bifurcation analysis	78
4.4. Numerical analysis	85
4.5. Hydranth regeneration in Tubularia	94



## CHAPTER I

### Introduction to Immobilized Enzyme Systems

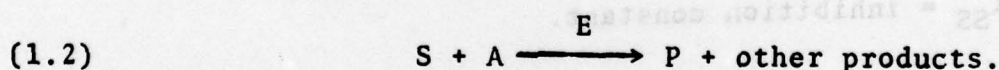
#### 1.1. What are enzymes?

Enzymes are catalysts of biochemical reactions.

In the simplest case typically, one reactant S, called a substrate, is consumed under the catalytic action of an enzyme E, and yields a product P.



For example, in such a reaction one might have E = glucose oxidase, S = glucose, P = gluconic acid. More than one substrate can be involved in the reaction. A second substrate is often called a cosubstrate. Similarly, more than one product can result from the reaction. For example, with S = uric acid, A = oxygen, E = uricase, P = allantoin, we can write



Generally, an enzyme catalyzes only a single type of reaction.

Enzyme kinetics have been studied since at least Michaelis and Menten [5] and a detailed description can be found in Dickson and Webb [6].

The rate expressions for enzyme reactions in a well-stirred solution vary greatly. One of the most simple is the monoenzyme irrever-

Accession For	WTIS G&H
DOC TAB	Unannounced
Justification	By
Distribution	Availability
Dist	Availability Codes
	Availand/or special

sible reaction rate expression

$$(1.3) \quad r = V_M \frac{[S]}{K_S + [S]}$$

Here  $K_S$  = Michaelis constant, characteristic of the enzyme;

$V_M$  = maximal reaction rate, proportional to enzyme concentration in the solution; and

$[S]$  = substrate concentration.

We shall deal with substrate inhibited phenomena for which the rate is given by

$$(1.4) \quad r = V_M \frac{[S]}{K_S + [S] (1 + \frac{[S]}{K_{SS}})}$$

Here  $K_{SS}$  = inhibition constant.

In the case of the reaction (1.2), the rate expression may be taken as

$$(1.5) \quad r = V_M \frac{[A]}{K_A + [A]} \frac{[S]}{K_S + [S] (1 + \frac{[S]}{K_{SS}})}$$

Here  $[A]$  = cosubstrate concentration and

$K_A$  = Michaelis constant of enzyme E for cosubstrate A.



If  $[A]$  is small with respect to  $[K_A]$ , we can approximate (1.5) by

$$(1.6) \quad r = V_M \frac{[A]}{K_A} \frac{[S]}{K_S + [S] (1 + \frac{[S]}{K_{SS}})}.$$

In the following we shall choose  $K_S$  as the unit of concentration, and use the dimensionless quantities

$$(1.7) \quad s = \frac{[S]}{K_S}, \quad a = \frac{[A]}{K_S}.$$

The rates of reaction (1.3), (1.4), (1.5), and (1.6) can then be written

$$(1.8) \quad r = V_M \frac{s}{1+s}$$

$$(1.9) \quad r = V_M \frac{s}{1+s+ks^2} \quad (k = \frac{K_S}{K_{SS}})$$

$$(1.10) \quad r = V_M \frac{a}{\lambda+a} \frac{s}{1+s+ks^2} \quad (k = \frac{K_S}{K_{SS}}, \lambda = \frac{K_A}{K_S})$$

$$(1.11) \quad r = V_M \frac{K_S}{K_A} a \frac{s}{1+s+ks^2}.$$

For a detailed discussion of enzyme kinetics, see Banks [7] and Murray [3].

### 1.2. What are immobilized enzymes?

In living cells, enzyme molecules are not in an homogeneous solution, but are linked to other protein molecules within a medium that is heterogeneous requiring the diffusion of metabolites (the substrates and the products). In other words there exist gradients of concentration, and the interaction of diffusion and enzyme reaction must be taken into account in the understanding of enzyme kinetics in living cells. Of course, the phenomena here are much more complicated. Other phenomena include convection, the possibility of electric fields due to ionized species, and the co-occurrence of many enzyme reactions, all of which make the study of a real cell very complicated.

Thus, the technology of artificial enzyme membranes has been developed (Thomas [8]): this enables one to study, in a well-defined context, basic phenomena due to the interaction of diffusion and enzyme reaction. Additional motivation lies in the potential use of artificial enzyme membranes for industrial, analytical and medical applications. We refer for a discussion of this aspect to Thomas [9].

By immobilized enzyme system we mean artificial membranes produced by linking enzyme molecules to inactive protein molecules, the whole forming a matrix where the enzyme is uniformly distributed. Such a membrane is a translucent film of about 50 $\mu$  thickness which is easily handled in the laboratory.

### 1.3. The "model case".

In the simplest case an artificial membrane  $M$  (slab geometry, Fig.1.1) separates 2 compartments  $C_0$  and  $C_1$ , containing substrate  $S$  at fixed concentrations  $s_0$  and  $s_1$ .  $S$  diffuses into  $M$  and, under the catalytic action of  $E$ , reacts: one molecule of  $E$  and one molecule of  $S$  combine to form a molecule of enzyme - substrate  $ES$ , which itself yields one molecule of product  $P$  and releases one molecule of enzyme  $E$ : schematically,

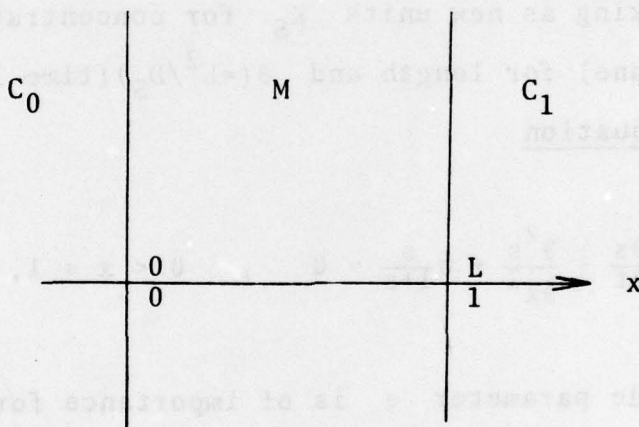
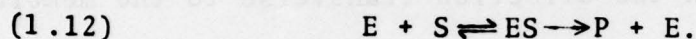


Figure 1.1

Thus, the net action of the enzyme is such that  $S$  disappears in the membrane with a rate given by (1.3). The local variation of substrate concentration within the membrane is due to



diffusion and reaction; this is expressed in the equation of continuity:

$$(1.13) \quad \frac{\partial [S]}{\partial t} - D_S \frac{\partial^2 [S]}{\partial x^2} + V_M \frac{[S]}{K_S + [S]} = 0.$$

Here  $[S]$  = concentration (moles  $\text{cm}^{-3}$ )

$t$  = time (hour)

$D_S$  = diffusion coefficient ( $\text{cm}^2 \text{h}^{-1}$ )

$x$  = abscissa in the direction transverse to the membrane (cm).

By taking as new units  $K_S$  for concentrations,  $L$  (thickness of the membrane) for length and  $\theta (= L^2/D_S)$  (time lag) for times, we obtain the equation

$$(1.14) \quad \frac{\partial s}{\partial t} - \frac{\partial^2 s}{\partial x^2} + \sigma \frac{s}{1+s} = 0, \quad 0 < x < 1, \quad t > 0$$

where the single parameter  $\sigma$  is of importance for the behavior of the membrane:

$$(1.15) \quad \sigma = \frac{V_M L^2}{K_S D_S} \quad (\text{square of the Thiele modulus}).$$

Equation (1.14) must be supplemented with boundary conditions

$$(1.16) \quad s(0, t) = s_0, \quad s(1, t) = s_1$$

and initial conditions; for example,

$$(1.17) \quad s(x,0) = 0$$

which corresponds to a membrane initially empty of any substrate.

The proof of existence and uniqueness of a (positive) solution for eqs. (1.14), (1.16), (1.17), as well as for the other equations of evolution presented in this chapter, can be found in Kernevez and Thomas [10].

Numerical simulations (using finite differences) produce an evolution of the profile of concentration tending to a stable steady state (Fig.1.2).

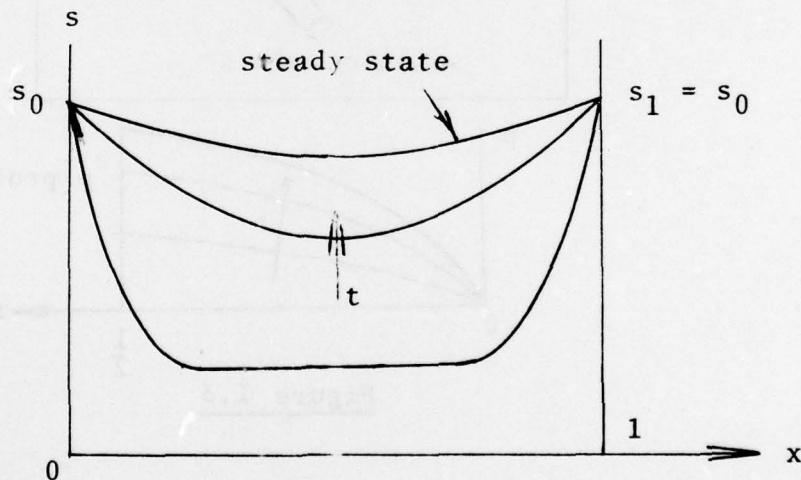


Figure 1.2

The main interest of this example is to demonstrate possibility of a fact which is not always taken into account: the existence of gradients of concentration in the interior of the membrane. Artificial membranes coupled with electrodes (an important configuration in many applications) also fall within this example: a membrane is attached to an electrode which is sensitive to the product  $P$  of the enzyme reaction (Fig. 1.3).

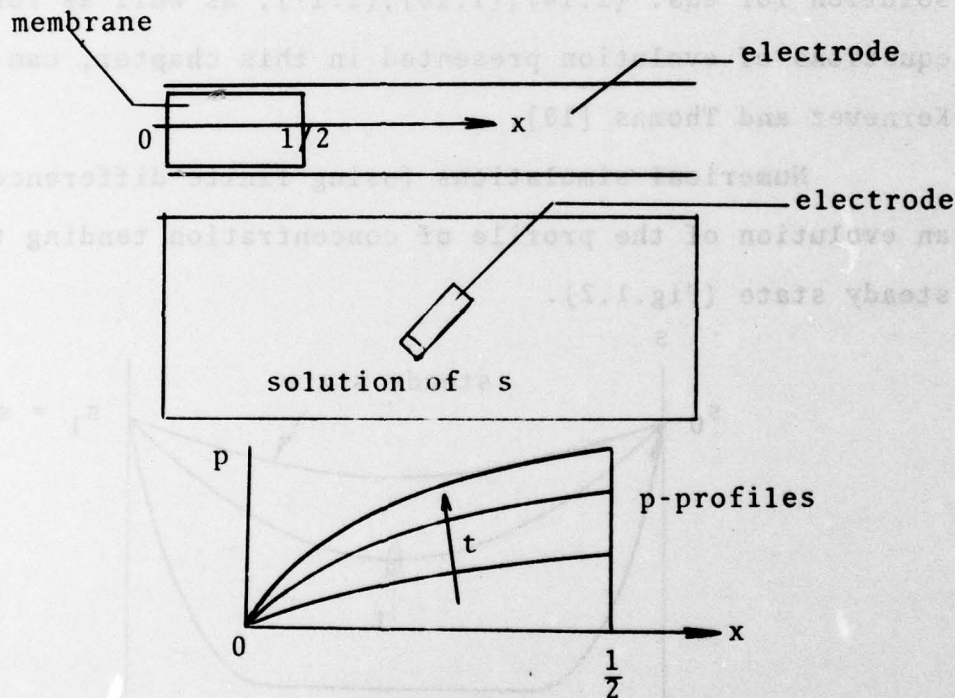


Figure 1.3

Due to the presence of the electrode, there is a zero-flux boundary condition at  $x = 1/2$  so that the  $S$  profiles evolve like the left half of the profiles in Fig. 1.2, whereas the  $P$ -profiles, governed by



$$(1.18) \quad \frac{\partial p}{\partial t} - \frac{D}{D_S} \frac{\partial^2 p}{\partial x^2} = \sigma \frac{s}{1+s}$$

$$(1.19) \quad p(0,t) = 0, \quad \frac{\partial p}{\partial x} = 0 \quad \text{for } x = \frac{1}{2}$$

$$(1.20) \quad p(x,0) = 0,$$

evolve, as depicted in Fig.1.3, towards a stable steady state. Of course in this example (1.16) has to be replaced by

$$(1.21) \quad s(0,t) = s_0, \quad \frac{\partial s}{\partial x}(\frac{1}{2},t) = 0.$$

From the measurement of the electrode one can get the concentration of  $P$  against the electrode, and hence the concentration of  $S$  at  $x = 0$ , that is, in the solution where the electrode is immersed. Due to the specificity of the enzyme, the electrode is specific for one particular substrate (glucose, saccharose, lactose, etc.). It is thus possible to monitor continuously the concentration of these substances in media like the blood or the broth of fermentations.

#### 1.4. The glucose pump. (Thomas et.al. [8])

In this example there is a spatial distribution of the enzymes and the interaction of diffusion and reaction creates a transport of  $S$  against a concentration gradient.

The membrane (Fig.1.4) consists of 2 layers, one with enzyme  $E_1$  (hexokinase) and the other with enzyme  $E_2$  (phosphatase).  $E_1$  transforms  $S$  (glucose) into  $P$  (glucose-6-phosphate) and  $E_2$  transforms  $P$  into  $S$ :

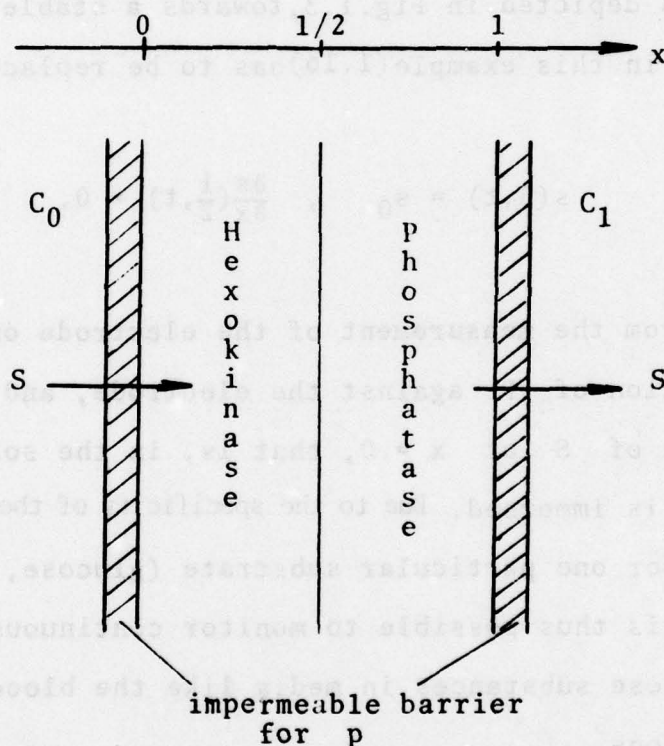
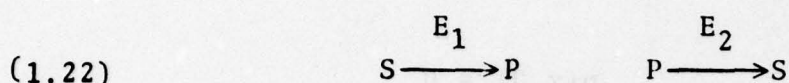


Figure 1.4

The membrane separates 2 compartments  $C_0$  and  $C_1$ , with substrate concentrations  $s_0$  and  $s_1$  ( $s_1 \geq s_0$ ). However, the



system pumps glucose from  $C_0$  to  $C_1$ . This is seen from the form of the  $S$  concentration profile (Fig.1.5).

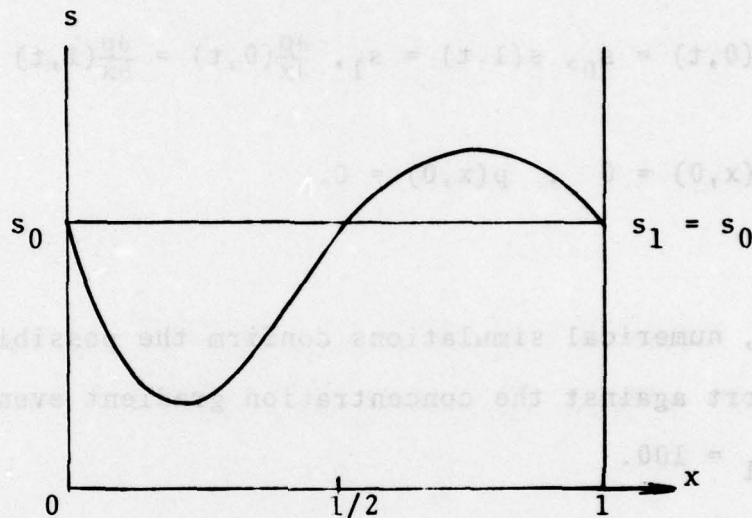


Figure 1.5

$S$  is consumed for  $0 < x < \frac{1}{2}$ ; its profile is convex.  $S$  is produced in the region  $\frac{1}{2} < x < 1$ ; its profile is concave. The flux of  $S$  at  $x = 0$  (resp.  $x = 1$ ) being given by  $-\frac{\partial S}{\partial x}(0,t)$  (resp.  $-\frac{\partial S}{\partial x}(1,t)$ ), we see that  $S$  is entering into the membrane at  $x = 0$ , and going out of it as  $x = 1$ . The result is an active transport of glucose from  $C_0$  to  $C_1$ ; this has been observed experimentally, and also is found when one solves numerically the corresponding equations:

$$\begin{aligned}
 (1.23) \quad & \left\{ \begin{aligned} & \frac{\partial s}{\partial t} - \frac{\partial^2 s}{\partial x^2} + r = 0, \quad \frac{\partial p}{\partial t} - \frac{\partial^2 p}{\partial x^2} - r = 0 \\ & r = \sigma \frac{s}{1+s+p} \quad \text{for } 0 < x < \frac{1}{2} \quad \text{and} \quad r = -\sigma \frac{p}{1+p} \quad \text{for } \frac{1}{2} < x < 1 \\ & s(0,t) = s_0, \quad s(1,t) = s_1, \quad \frac{\partial p}{\partial x}(0,t) = \frac{\partial p}{\partial x}(1,t) = 0 \\ & s(x,0) = 0, \quad p(x,0) = 0. \end{aligned} \right.
 \end{aligned}$$

Indeed, numerical simulations confirm the possibility of active transport against the concentration gradient even for  $s_0 = 1$  and  $s_1 = 100$ .

### 1.5. Substrate inhibited kinetics.

All the systems to be studied henceforth will be endowed with substrate inhibited kinetics:

(i) systems for which multiple steady states may exist.

$$\begin{aligned}
 (1.24) \quad & \left\{ \begin{aligned} & \frac{\partial s}{\partial t} - \frac{\partial^2 s}{\partial x^2} + \sigma \frac{s}{1+s+ks^2} = 0, \quad 0 < x < 1, \quad t > 0 \\ & s(0,t) = s_0, \quad s(1,t) = s_1 \\ & s(x,0) = \text{fixed.} \end{aligned} \right.
 \end{aligned}$$

These equations represent the evolution of substrate concentrations

in a membrane separating 2 compartments with fixed concentrations  $s_0$  and  $s_1$  (Fig.1.1). We have not specified the given initial profile of concentration  $x \rightarrow s(x,0)$  but, as we shall see in chapter 2, the steady state will depend upon it.  $\sigma$  and  $k$  have been defined in (1.15) and (1.9).

(ii) systems for which periodic oscillations in time may exist.

$$(1.25) \quad \begin{cases} \frac{\partial s}{\partial t} - \frac{\partial^2 s}{\partial x^2} + \sigma a \frac{s}{1+s+ks^2} = 0, & 0 < x < 1, \quad t > 0 \\ \frac{\partial a}{\partial t} - \alpha \frac{\partial^2 a}{\partial x^2} + \sigma a \frac{s}{1+s+ks^2} = 0 \\ s(0,t) = s_0, \quad s(1,t) = s_1, \quad a(0,t) = a_0, \quad a(1,t) = a_1. \end{cases}$$

Here the rate of reaction is that given in (1.11) and

$$(1.26) \quad \sigma = \frac{V_M}{K_A} \frac{L^2}{D_S}, \quad \alpha = \frac{D_A}{D_S},$$

where  $D_A$  is the diffusion coefficient for A. (Though  $a$  is the concentration of a cosubstrate A, we denote it by  $a$  because A acts like an activator in the reaction.)

(iii) the S - A system.

We consider a reaction such as (1.2), with rate (1.6) taking place in an active layer (i.e. the enzyme is immobilized within it). This active layer is thin enough to be considered as



a planar domain  $\Omega$  (Fig.1.6) where the concentrations of  $S$  and  $A$  depend on the position in  $\Omega$  but not on the position in the transverse direction. An inactive (i.e. without enzyme)

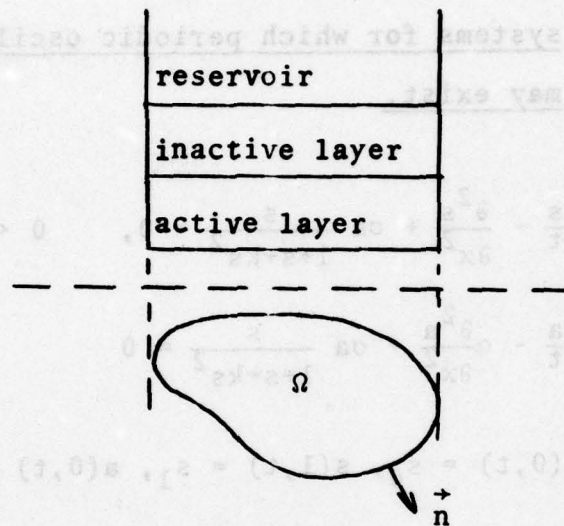


Figure 1.6

boundary layer separates  $\Omega$  from an outside well-stirred reservoir where  $S$  and  $A$  are at fixed concentrations  $S_0$  and  $A_0$ . In  $\Omega$  3 phenomena take place: transport from the reservoir through the inactive layer, diffusion and reaction. The balance of masses for  $S$  can be written

$$(1.27) \quad L_1 \left( \frac{\partial [S]}{\partial t} - D_S \left( \frac{\partial^2 [S]}{\partial x^2} + \frac{\partial^2 [S]}{\partial y^2} \right) + v_M \frac{[A]}{K_A} \frac{[S]}{K_S + [S] (1 + \frac{[S]}{K_{SS}})} \right) - D_S' \frac{S_0 - [S]}{L_2} = 0.$$

Here  $L_1$  (resp.  $L_2$ ) is the thickness of the active (resp. inactive) layer, and  $D_S$  (resp.  $D'_S$ ) is the diffusion coefficient of  $S$  in the active (resp. inactive) layer.

Taking as new units  $L$  (diameter of  $\Omega$ ) for length,  $\theta$  ( $= L^2/D_S$ ) for time and  $K_S$  for concentrations we obtain

$$(1.28) \quad \frac{\partial s}{\partial t} - \Delta s + \sigma a \frac{s}{1+s+ks^2} - \gamma(s_0-s) = 0.$$

Here  $\Delta$  is the 2-dimensional Laplacian,  $\sigma = \frac{V_M}{K_A} \theta$  and  $\gamma = \theta/\theta'$  ( $\theta' = L_1 L_2 / D'_S$ ). Similarly for  $A$  we find

$$(1.29) \quad \frac{\partial a}{\partial t} - \beta \Delta a + \sigma a \frac{s}{1+s+ks^2} - \alpha \gamma (a_0 - a) = 0,$$

where  $\alpha = \frac{D'_A}{D'_S}$  and  $\beta = \frac{D_A}{D_S}$  are the ratios of the diffusion coefficients for  $A$  and  $S$  in the inactive and active layers.

Equations (1.28) and (1.29) are supplemented with zero flux boundary conditions:

$$(1.30) \quad \frac{\partial s}{\partial n} = 0 \quad \text{and} \quad \frac{\partial a}{\partial n} = 0$$

( $\frac{\partial s}{\partial n} = \vec{n} \cdot \vec{\nabla} s$ ,  $\vec{n}$  being the unit normal to  $\partial\Omega$  pointing outwards). As usual, initial conditions for  $s$  and  $a$  have to be specified. We shall deal with the  $S - A$  system in chapter 3 for wave front propagation, and in chapter 4 for pattern formation. There we

shall be mainly interested in its steady states. The S - A system more generally can be the modelling of diffusion and enzyme reaction on a surface separated from an external medium by a boundary layer. The Laplace-Beltrami operator  $\Delta_B$  is then appropriate to represent diffusion on the surface, and the S - A system equations are

$$(1.31) \quad \begin{cases} \frac{\partial s}{\partial t} - \Delta_B s + \sigma F(s, a) - \gamma(s_0 - s) = 0 \\ \frac{\partial a}{\partial t} - \beta \Delta_B a + \sigma F(s, a) - \alpha \gamma(a_0 - a) = 0 \\ F(s, a) = as/(1+s+ks^2) \end{cases}$$

with no boundary conditions if the surface is closed.

Let us recall the definition of <sup>the</sup> Laplace Beltrami operator: locally the surface (think of a cucumber surface!) can be mapped into the interior of a square:  $-1 < u_1 < +1$ ,  $-1 < u_2 < +1$  (Fig.1.7)

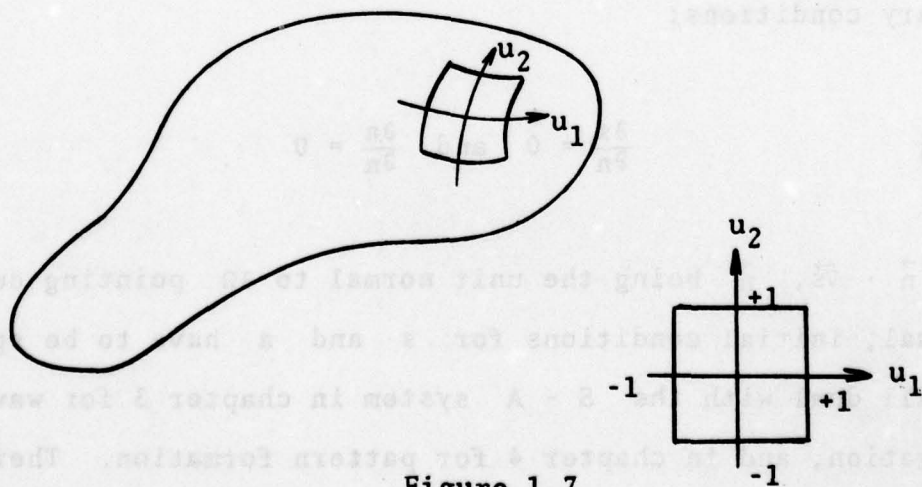


Figure 1.7



and  $x, y, z$  coordinates on  $S$  can be expressed as

$$(1.32) \quad x = x(u_1, u_2), \quad y = y(u_1, u_2), \quad z = z(u_1, u_2).$$

Define

$$(1.33) \quad d\ell^2 = dx^2 + dy^2 + dz^2 = a_{11}du_1^2 + 2a_{12}du_1du_2 + a_{22}du_2^2,$$

$$(1.34) \quad a = a_{11}a_{22} - a_{12}^2,$$

$$(1.35) \quad a^{11} = \frac{a_{22}}{a}, \quad a^{22} = \frac{a_{11}}{a}, \quad a^{12} = a^{21} = -\frac{a_{12}}{a}.$$

Then

$$(1.36) \quad ds = a^{1/2} du_1 du_2$$

$$(1.37) \quad \Delta_B \phi = \frac{1}{a^{1/2}} \sum_{\alpha, \beta} \frac{\partial}{\partial u_\beta} (a^{1/2} a^{\alpha\beta} \frac{\partial \phi}{\partial u_\alpha})$$

$$(1.38) \quad \int_S (-\Delta_B \phi) \psi ds = \int_S a^{\alpha\beta} \frac{\partial \phi}{\partial u_\alpha} \frac{\partial \psi}{\partial u_\beta} dS.$$

As we shall see in chapter 4, it is no more difficult to solve numerically the  $S - A$  system on a cucumber surface than on a planar surface by using the finite element method. However, there we shall have in mind the surface of an egg rather than the surface of a cucumber!

## CHAPTER II

Multiple Steady States and Hysteresis2.1. The 0-dimensional case.

The equation

$$(2.1) \quad \frac{ds}{dt} = s_0 - s - \rho F(s)$$

represents the rate of change of the substrate concentration  $s$  in a well-stirred cell (Fig.2.1) where a substrate inhibited reaction takes place:

$$(2.2) \quad F(s) = \frac{s}{1+s+ks^2}$$

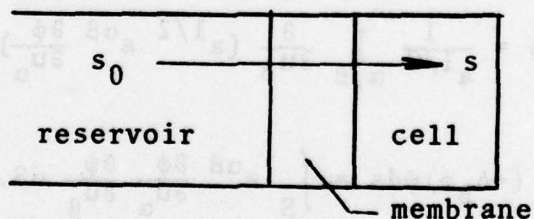


Figure 2.1

The cell is separated from a well stirred reservoir with fixed concentration  $s_0$  by an inactive (i.e. without enzyme) membrane transporting the substrate by diffusion from the reservoir to the



cell with a flux  $s_0 - s$ . In this system diffusion and (enzyme) reaction take place in distinct spatial regions; however, it is one of the simplest imaginable systems in which the coupling of reaction and diffusion yields a phenomenon involving multiple steady states; in this case governed by solutions of

$$(2.3) \quad s_0 - s = \rho F(s).$$

In fact, it is also an open system, due to the transport into the system with a flux  $s_0 - s$ . Without this transport from outside, the system would evolve, according to the kinetic equation

$$(2.4) \quad \frac{ds}{dt} = -\rho F(s),$$

to the equilibrium state  $s = 0$ . But equation (2.2) possesses solutions "far from this equilibrium", simply obtained by cutting the curve  $y = \rho F(s)$  by the straight line  $y = s_0 - s$  (Fig.2.2).

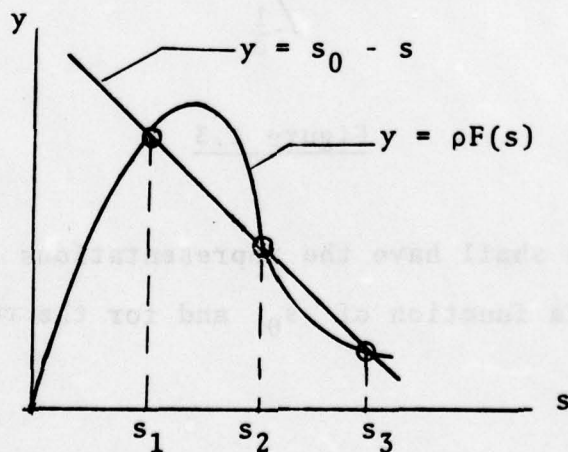


Figure 2.2 - solutions of (2.2).

If we fix  $\rho$  in (2.3) and wish to get  $s$  as a (possibly multivalued) function of  $s_0$ , we can consider the graphs of  $s \rightarrow s_0 = s + \rho F(s)$  (Fig. 2.3) and of  $s \rightarrow F'(s)$  where it is easily seen that if  $\rho > -1/\min F'(s)$ , there are 2 values  $s^*$  and  $s^{**}$  of  $s$  such that  $\frac{ds_0}{ds} = 1 + \rho F'(s) = 0$ , and  $s_0 = s + \rho F(s)$  admits relative extrema.

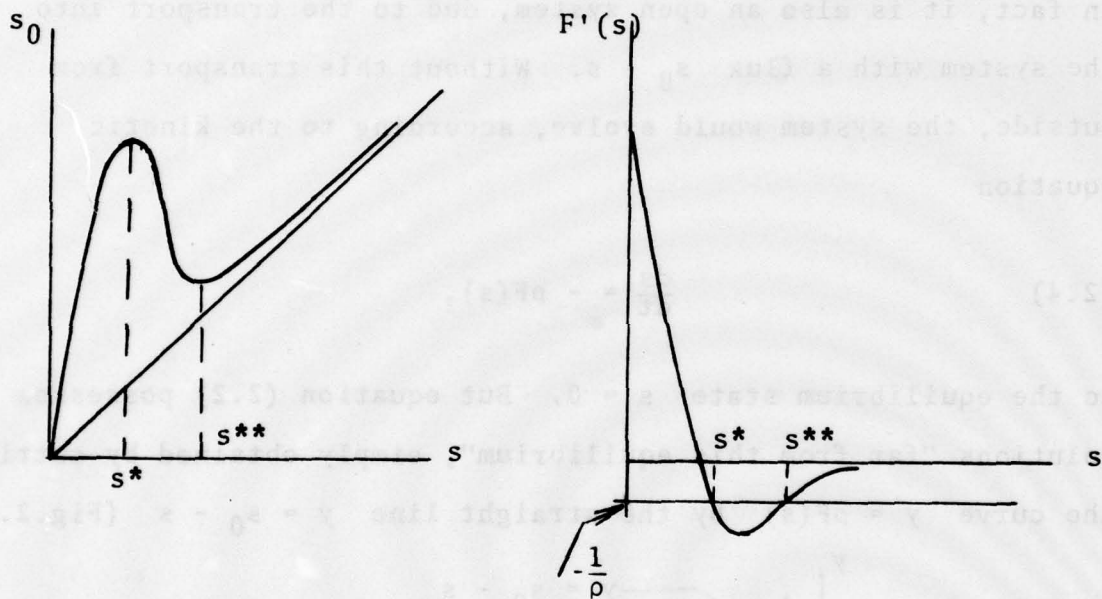


Figure 2.3

In that case we shall have the representations depicted in Fig. 2.4 for  $s$  as a function of  $s_0$  and for the reaction rate of the system:

$$(2.5) \quad r = s_0 - s = \rho F(s).$$

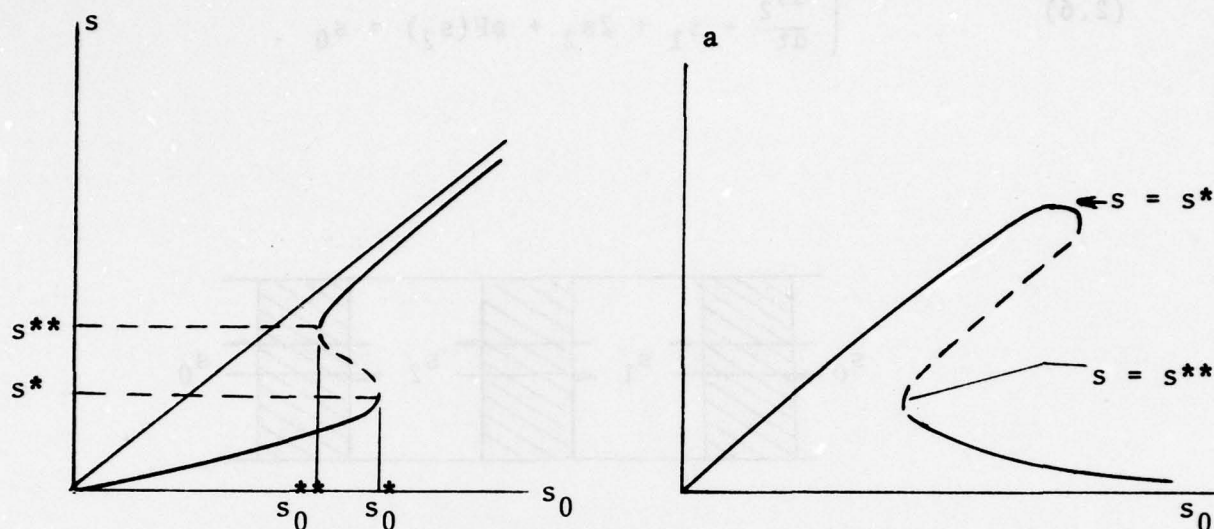


Figure 2.4

All of the above is easily seen, as is the stability of the state  $s$  with respect to the dynamical system (2.1) which changes when  $1 + \rho F'(s)$  changes sign, i.e. at the turning points  $s = s^*$  and  $s = s^{**}$ . However, the behavior of the simple system shown in Fig. 2.4 will extend to more complex cases, e.g. distributed systems.

The 0-dimensional case: 2 cells. (Bunow et.al. [11])

We consider now 2 cells, (see Fig. 2.5), where the substrate concentrations  $s_1$  and  $s_2$  are governed by



$$(2.6) \quad \begin{cases} \frac{ds_1}{dt} + 2s_1 - s_2 + \rho F(s_1) = s_0 \\ \frac{ds_2}{dt} - s_1 + 2s_2 + \rho F(s_2) = s_0 \end{cases}$$

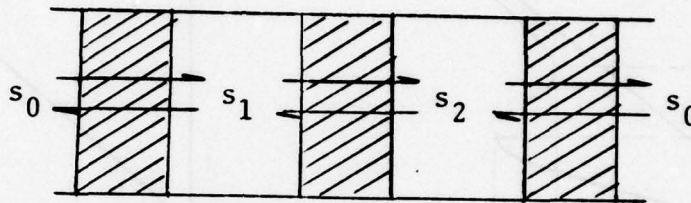


Figure 2.5

A first branch of solutions of the steady state equations

$$(2.7) \quad \begin{cases} 2s_1 - s_2 + \rho F(s_1) = s_0 \\ -s_1 + 2s_2 + \rho F(s_2) = s_0 \end{cases}$$

consists of "symmetric solutions"  $s_1 = s_2 = s$ , with (2.3). But there may exist "non symmetric" steady states  $(s_1 \neq s_2)$ , as follows from the stability study of the symmetric states  $(s_1, s_2) = (s, s)$ : the linearized operator

$$\begin{bmatrix} 2+\rho F'(s_1) & -1 \\ -1 & 2+\rho F'(s_2) \end{bmatrix} = \begin{bmatrix} 2+\rho F'(s) & -1 \\ -1 & 2+\rho F'(s) \end{bmatrix}$$

has eigenvalues  $\lambda_1 = 1 + \rho F'(s)$  and  $\lambda_2 = 3 + \rho F'(s)$ . Thus in addition to the turning points  $(s_0^*, s^*, s^*)$  and  $(s_0^{**}, s^{**}, s^{**})$  corresponding to  $\lambda_1 = 0$ , one may have, if  $\rho$  is large enough,  $\lambda_2 = 0$  (Fig. 2.6), and consequently a bifurcation point. As the reaction rate is the same for 2 "mirror states"  $(s_1, s_2)$  and  $(s_2, s_1)$ ,

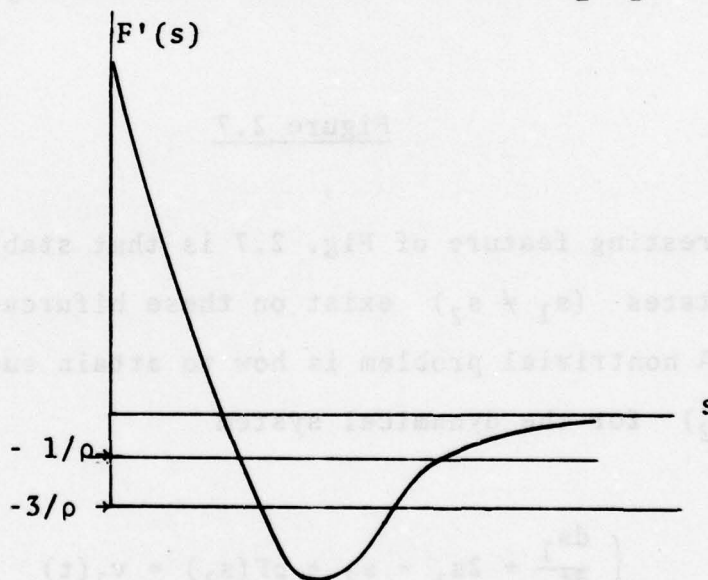


Figure 2.6

the reaction rate of the two bifurcated states will be represented by only one curve (Fig. 2.7).

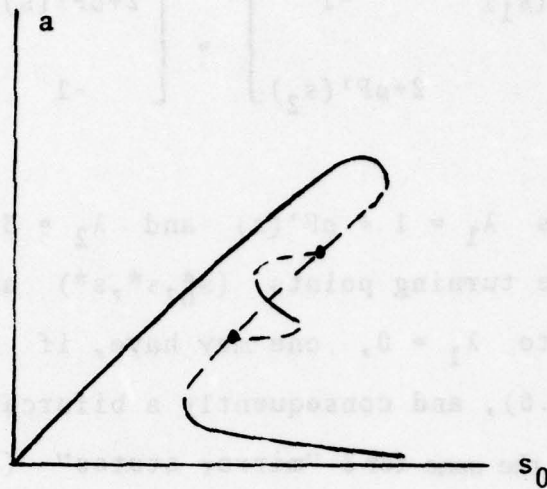


Figure 2.7

One interesting feature of Fig. 2.7 is that stable non-uniform steady states  $(s_1 \neq s_2)$  exist on these bifurcated branches.

A nontrivial problem is how to attain such a N.U.S.S.  $(\tilde{s}_0, \tilde{s}_1, \tilde{s}_2)$  for the dynamical system

$$(2.8) \quad \begin{cases} \frac{ds_1}{dt} + 2s_1 - s_2 + \rho F(s_1) = v_1(t) \\ \frac{ds_2}{dt} - s_1 + 2s_2 + \rho F(s_2) = v_2(t) \end{cases}$$

or for a sequence of steady states  $(s_1, s_2)$



$$(2.9) \quad \begin{cases} 2s_1 - s_2 + \rho F(s_1) = v_1(t) \\ -s_1 + 2s_2 + \rho F(s_2) = v_2(t) \end{cases}$$

In both cases we should have, at some given time  $T$ ,

$$(2.10) \quad s_1(T) = \tilde{s}_1, s_2(T) = \tilde{s}_2, v_1(T) = v_2(T) = \tilde{s}_0.$$

### Imperfection

If, instead of (2.7), one has

$$(2.10a) \quad \begin{cases} 2s_1 - s_2 + \rho F(s_1) = s_0 \\ -s_1 + 2s_2 + \rho F(s_2) = s_0 + \epsilon \end{cases}$$

then we have no more a bifurcation, but, in Fig. 2.7, a "lemniscate" detaches from the main branch (Fig. 2.8).

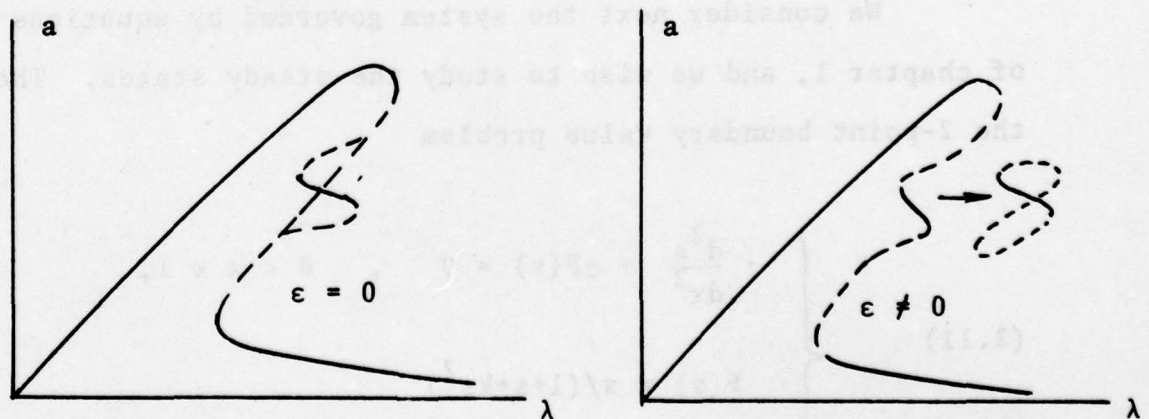


Figure 2.8

This lemniscate comes in part from one of the bifurcated branches and in part from the arc of symmetric states. It is an example of "imperfection" (Fig. 2.9).

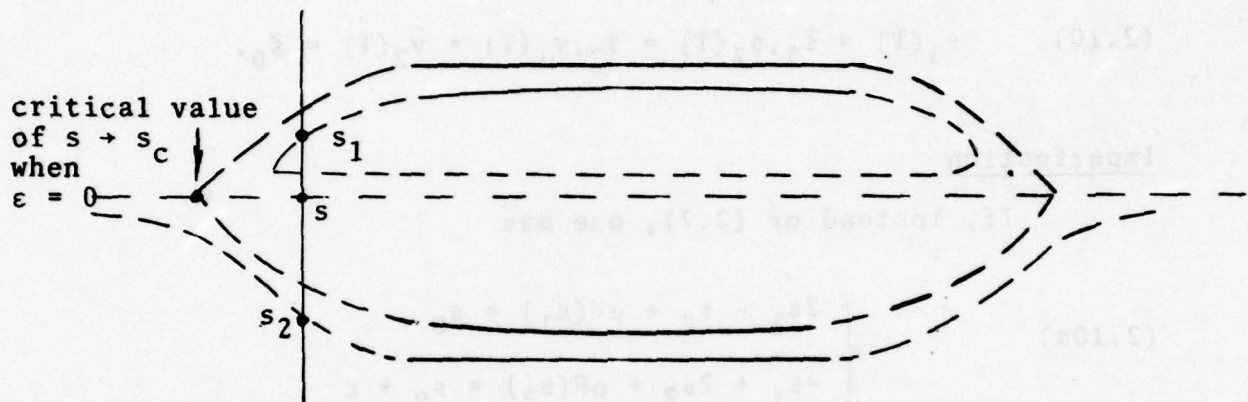


Figure 2.9

## 2.2. 1-dimensional case.

We consider next the system governed by equations (1.24) of chapter 1, and we wish to study the steady states. They satisfy the 2-point boundary value problem

$$(2.11) \quad \left\{ \begin{array}{l} -\frac{d^2 s}{dx^2} + \sigma F(s) = 0 \quad , \quad 0 < x < 1, \\ F(s) = s/(1+ks^2) \\ s(0) = s(1) = s_0. \end{array} \right.$$



Here we take  $s(0) = s(1)$  in order to simplify the analysis.

Problem (2.11) has a first integral

$$(2.12) \quad -s'^2(x) + 2\sigma G(s(x)) = 2\sigma G(\mu)$$

where  $G$  is the indefinite integral of  $F(G'=F)$  and  $\mu = s(1/2)$ .

(Since  $s'' > 0$ ,  $s$  is a convex function of  $x$ , and since

$s(0) = s(1)$  the  $s$  profile is symmetric with respect to  $x = \frac{1}{2}$ .)

Moreover, if we restrict our considerations to  $\frac{1}{2} < x < 1$ ,  $s'(x) > 0$  so that

$$\frac{ds}{dx} = (2\sigma)^{1/2} (G(s) - G(\mu))^{1/2}$$

and

$$(2.13) \quad (2\sigma)^{1/2} (x - \frac{1}{2}) = \int_{\mu}^{s(x)} \frac{d\xi}{(G(\xi) - G(\mu))^{1/2}} .$$

The solution of (2.11) is equivalent to the solution of (2.13) together with the condition requiring  $s(1) = s_0$ :

$$(2.14) \quad (\frac{\sigma}{2})^{1/2} = \int_{\mu}^{s_0} \frac{d\xi}{(G(\xi) - G(\mu))^{1/2}} .$$

In fact (2.11) has as many solutions as we can find several values

of  $\mu$  satisfying (2.14), or

$$(2.15) \quad f(\mu) = \left(\frac{\sigma}{2}\right)^{1/2}$$

where

$$(2.16) \quad f(\mu) = \int_{\mu}^{s_0} \frac{d\xi}{(G(\xi) - G(\mu))^{1/2}}$$

It can be shown (Kernevez [10]) that for  $s_0$  large enough the graph of  $f$  has the shape indicated in Fig. 2.10, so that there are 3 solutions to (2.15) if  $\sigma$  is in a suitable interval.

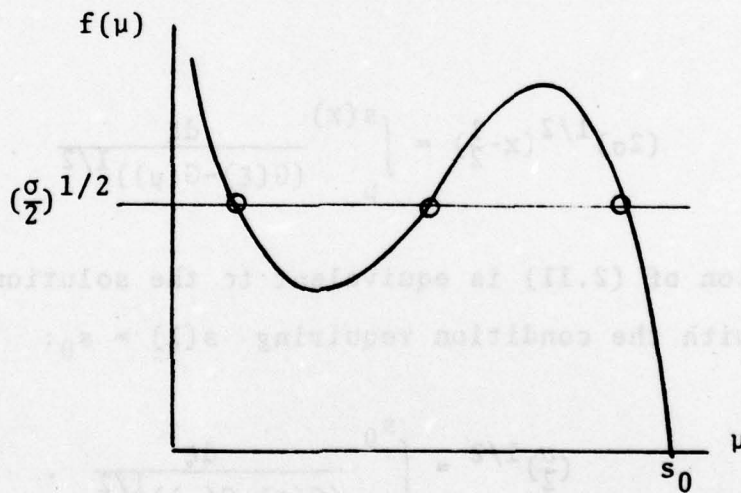


Figure 2.10

The upper and lower solutions can be easily obtained numerically by using the following scheme:

- (i) start from  $s^0(x) = s_0$  for the upper solution and  $s^0(x) = 0$  for the lower solution:
- (ii) define  $s^{(k+1)}(x)$  from  $s^{(k)}(x)$  by

$$(2.17) \quad \begin{cases} -\frac{d^2 s^{(k+1)}(x)}{dx^2} + \sigma \frac{1}{1+s^{(k)}(x)+ks^{(k)}(x)^2} s^{(k+1)}(x) = 0 \\ s^{(k+1)}(0) = s^{(k+1)}(1) = s_0, \end{cases}$$

and iterate until

$$(2.18) \quad \max |s^{(k+1)}(x) - s^{(k)}(x)| < \epsilon.$$

One thus obtains two stable steady states for the same boundary value  $s_0$  (Fig. 2.11).

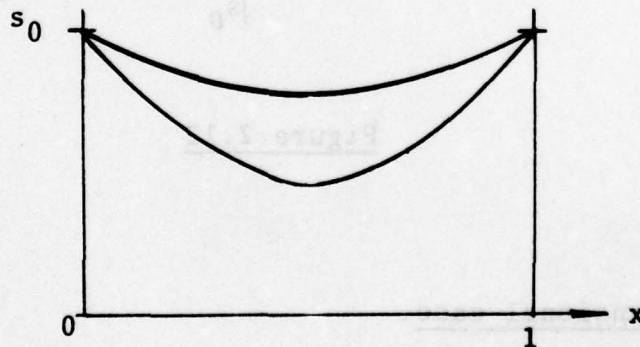


Figure 2.11



For a detailed study of the multiple steady states in the one-dimensional case we refer to Brauner and Nicolaenko [12]. The curve which represents  $\mu(=s(\frac{1}{2}))$  as a function of  $s_0(=s(0)=s(1))$  is similar to the one in Fig. 4. Hysteresis may be observed for a given boundary value  $s_0$  the system can be in one of two possible stable states depending on its past history. Thus we have a simple model of a system with memory (see Fig. 2.12).

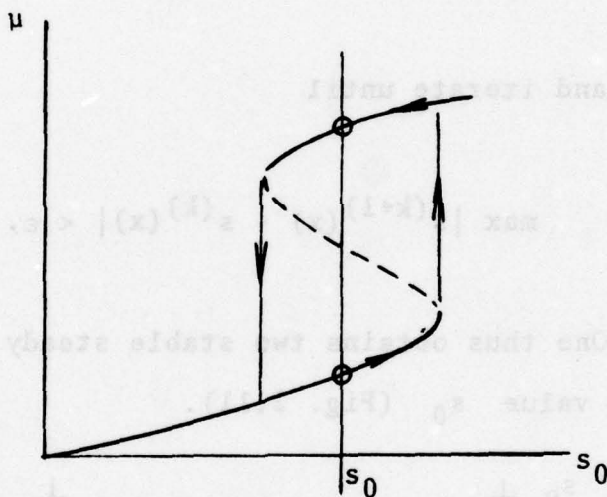


Figure 2.12

### 2.3. 2-dimensional case.

We are interested in the steady states defined by

$$(2.19) \quad \begin{cases} -\Delta s + \sigma F(s) = 0 & \text{in } \Omega \\ F(s) = s/(1+s+ks^2) \\ s|_{\Gamma} = s_0 \end{cases}$$

where  $\Omega$  is a bounded set in  $\mathbb{R}^2$  or  $\mathbb{R}^3$ . Brauner and Nicolaenko [13] have demonstrated the possibility of multiple solutions for (2.19). Their proof uses a regular perturbation method: equation (2.19) can be rewritten

$$(2.20) \quad \begin{cases} -\Delta u + \frac{u}{\epsilon^2 + \beta \epsilon u + k \beta^2 u^2} = 0 \\ u|_{\Gamma} = 1 \end{cases}$$

by defining  $u = s/s_0$ ,  $\epsilon^2 = \frac{1}{\sigma}$ ,  $\beta = s_0 \epsilon$ .

We have already made the remark that in order to obtain multiple steady states we must have  $\sigma$  and  $s_0$  sufficiently large. Therefore, the hypothesis  $\sigma = \frac{1}{\epsilon^2}$  and  $s_0 = \frac{\beta}{\epsilon}$  seems reasonable, and in fact in the one-dimensional case, typical values for which there are multiple states are  $\sigma = 1200$ ,  $s_0 = 72$ , corresponding to  $\epsilon \simeq \frac{1}{32}$ ,  $\beta \simeq 2.2$ .

Brauner and Nicolaenko prove the following:

(i) there exists a branch of maximal solutions to

$$\begin{cases} -\Delta u + \frac{1}{k\beta^2 u} = 0 \\ u|_{\Gamma} = 1 \end{cases}$$

with a turning point  $T$  (Fig. 2.13),

- (ii) for  $\epsilon$  small enough, the same is true for (2.20), with turning point  $T_1$ ,
- (iii) there is at least one other turning point  $T_2$  for (2.20).

Because of the difficulty in obtaining theoretical results on the qualitative behavior of the solution of equations such as (2.19), it is interesting to develop efficient algorithms to follow the branch of solutions when a parameter like  $s_0$  varies. Such an algorithm is described in the next section.

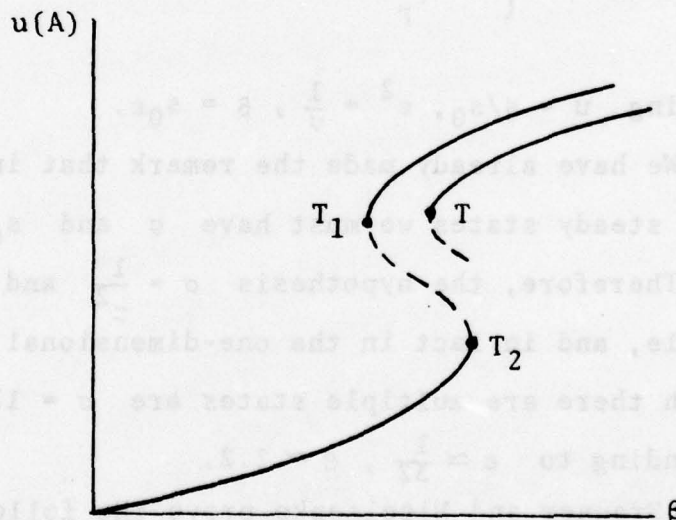


**Figure 2.13**

Graph of  $u(A)$ ,  $A$  being any point in  $\Omega$ .



#### 2.4. Numerical analysis.

A finite element discretization of (2.19) gives an equation of the form

$$(2.21) \quad F(x, \lambda) = 0.$$

Here  $\lambda = s_0$ ,  $x = [x_1, x_2, \dots, x_N]^T$  is the vector of (unknown) nodal values and

$$(2.22) \quad F(x, \lambda) = [F_1(x, \lambda), F_2(x, \lambda), \dots, F_N(x, \lambda)]^T$$

so that in fact (2.21) is a set of  $N$  (non-linear) equations of  $N$  unknowns depending upon the parameter  $\lambda$ .

The method of Kubicek [14] consists of solving the constrained system

$$(2.23) \quad \begin{cases} F(x(t), \lambda(t)) = 0 \\ \left(\frac{dx}{dt}\right)^2 + \left(\frac{d\lambda}{dt}\right)^2 = 1, \end{cases}$$

where  $t$  is the arclength on the curve of solutions. This is equivalent to solving the differential equations

$$(2.24) \quad \begin{cases} \frac{\partial F}{\partial x} \frac{dx}{dt} + \frac{\partial F}{\partial \lambda} \frac{d\lambda}{dt} = 0 \\ \left(\frac{dx}{dt}\right)^2 + \left(\frac{d\lambda}{dt}\right)^2 = 1, \end{cases}$$

for which we can employ any numerical method (Euler, Adams-Bashforth, ...) if we are able to calculate  $\frac{dx}{dt}$  and  $\frac{d\lambda}{dt}$ .

We can proceed in the following way:

(i) Solve

$$(2.25) \quad \frac{\partial F}{\partial x} y = - \frac{\partial F}{\partial \lambda}.$$

(ii) We know that  $\frac{dx}{d\lambda} = \frac{d\lambda}{dt} y$ . Replace in the 2nd equation of (2.24):

$$(2.26) \quad (|y|^2 + 1) \left( \frac{d\lambda}{dt} \right)^2 = 1, \quad \frac{d\lambda}{dt} = \frac{\pm 1}{\sqrt{|y|^2 + 1}}$$

Suppose, for example, that we are on an arc of the curve where  $\frac{d\lambda}{dt} > 0$ . Then  $\frac{d\lambda}{dt}$  is known and hence  $\frac{dx}{dt}$ .

(iii) The application of Euler method for instance will make the point  $(x, \lambda)$  move from  $M_1$  to  $M_2$  (Fig. 2.14).

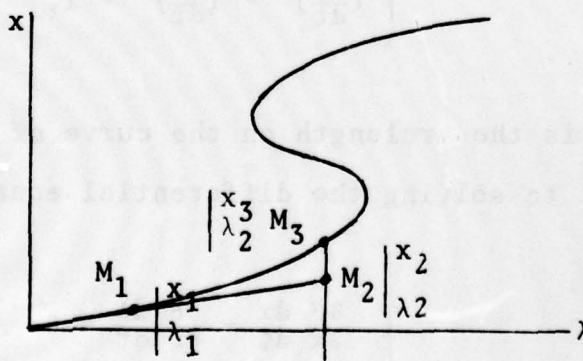


Figure 2.14

(iv) The Newton-Raphson method or the secant method applied to (2.21) will then give  $M_3$  on the curve. The drawback of this method is that when one approaches a turning point, the jacobian  $\frac{\partial F}{\partial x}$ , which can be monitored by its determinant, has a tendency to become singular. As we need to solve (2.25) and linear systems with the same matrix  $\frac{\partial F}{\partial x}$  for Newton's method, we have to check whether its determinant is not too small. If it is, then we have to interchange a spatial variable ( $x_N$ , for instance) and  $\lambda$ : the first equation of (2.24) can be written

$$(2.27) \quad \begin{bmatrix} \frac{\partial F'}{\partial x'} & \frac{\partial F'}{\partial x_N} \\ \frac{\partial F_N}{\partial x'} & \frac{\partial F_N}{\partial x_N} \end{bmatrix} \begin{bmatrix} \frac{dx'}{dt} \\ \frac{dx_N}{dt} \end{bmatrix} + \begin{bmatrix} \frac{\partial F'}{\partial \lambda} \\ \frac{\partial F_N}{\partial \lambda} \end{bmatrix} \frac{d\lambda}{dt} = 0.$$

Here  $x' = [x_1 x_2 \dots x_{N-1}]^T$ ,  $F' = [F_1 \dots F_{N-1}]^T$ .

$$(2.28) \quad \begin{cases} \frac{\partial F'}{\partial x'} \frac{dx'}{dt} + \frac{\partial F'}{\partial x_N} \frac{dx_N}{dt} + \frac{\partial F'}{\partial \lambda} \frac{d\lambda}{dt} = 0 \\ \frac{\partial F_N}{\partial x'} \frac{dx'}{dt} + \frac{\partial F_N}{\partial x_N} \frac{dx_N}{dt} + \frac{\partial F_N}{\partial \lambda} \frac{d\lambda}{dt} = 0, \end{cases}$$

or

$$(2.29) \quad \begin{bmatrix} \frac{\partial F'}{\partial x'} & \frac{\partial F'}{\partial \lambda} \\ \frac{\partial F_N}{\partial x'} & \frac{\partial F_N}{\partial \lambda} \end{bmatrix} \begin{bmatrix} \frac{dx'}{dt} \\ \frac{d\lambda}{dt} \end{bmatrix} + \begin{bmatrix} \frac{\partial F'}{\partial x_N} \\ \frac{\partial F_N}{\partial x_N} \end{bmatrix} \frac{dx_N}{dt} = 0.$$



Solving (2.29) together with the 2nd equation of (2.24), or solving (2.24), are similar problems. We essentially have in each case to solve a system of the form

$$(2.30) \quad \begin{bmatrix} A_{11} & A_{12} \\ A_{21} & A_{22} \end{bmatrix} \begin{bmatrix} y_1 \\ y_2 \end{bmatrix} = \begin{bmatrix} f_1 \\ f_2 \end{bmatrix}$$

where  $A_{11}$  is always the same  $(N-1) \times (N-1)$  matrix  $\frac{\partial F'}{\partial x'}$ ,  $A_{12}$  is  $(N-1) \times 1$ ,  $A_{21}$  is  $1 \times (N-1)$  and  $A_{22} \in \mathbb{R}$ . We want to take advantage of the fact that  $A_{11}$  is symmetric and sparse and use skyline storage for it together with an efficient solver (Bathe and Wilson [15]). Suppose that we have already made the triangularization of  $A_{11}$ :  $A_{11} = LDL^T$ . We observe that

$$A_{11}y_1 + A_{12}y_2 = f_1, \quad y_1 = A_{11}^{-1}f_1 - A_{11}^{-1}A_{12}y_2.$$

But  $c_1 = A_{11}^{-1}f_1$  and  $c_2 = A_{11}^{-1}A_{12}$  can be found by solving

$$(2.31) \quad A_{11}c_1 = f_1$$

and

$$(2.32) \quad A_{11}c_2 = A_{12}.$$

Now replace  $y_1$  by  $c_1 - y_2 c_2$  in the 2nd equation of  
 (2.30) ( $A_{22}$ ,  $y_2$  and  $f_2$  are numbers):

$$A_{21}c_1 - y_2 A_{21}c_2 + A_{22}y_2 = f_2$$

Hence,

(2.33)

$$y_2 = \frac{f_2 - A_{21}c_1}{A_{22} - A_{21}c_2}$$

$$y_1 = c_1 - y_2 c_2$$

## 2.5. Optimum design.

We shall investigate the dependence of solutions of (2.19) upon the geometrical domain  $\Omega$ , using methods of Murat and Simon [16], Mignot, Murat and Puel [17].

For a given domain  $\Omega$  and a given value of  $\sigma$  we know that the activity

$$(2.34) \quad a = \int_{\Gamma} \frac{\partial s}{\partial n} dt = \sigma \int_{\Omega} F(s) dx$$

varies with  $s_0$  as indicated in figure 2.15. We are interested in the value of  $s_0$  for which the activity is maximum.

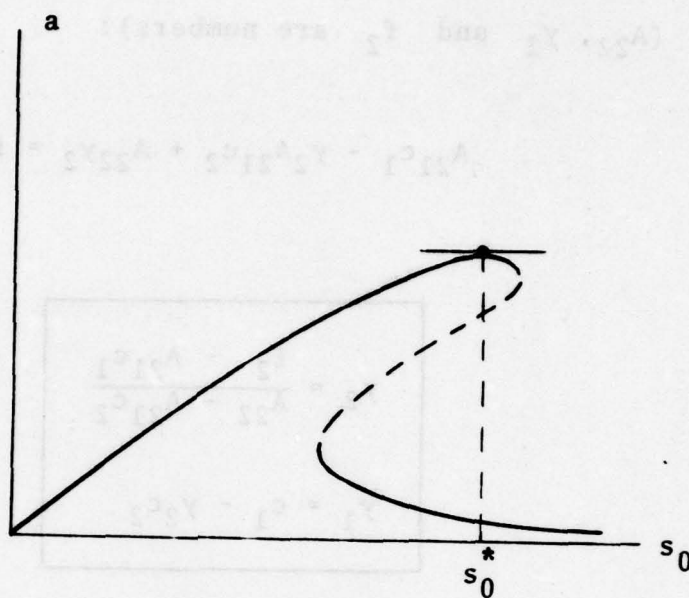


Figure 2.15

In the following  $s_0^*$  and  $s^*$  will denote this  $s_0$  (a number) and the corresponding state

$$(2.35) \quad -\Delta s^* + \sigma F(s^*) = 0, \quad s^*|_{\Gamma} = s_0^*$$

$$(2.36) \quad \frac{da}{ds_0} = 0 \quad \text{or} \quad \int_{\Gamma} \frac{\partial S}{\partial n} d\Gamma = 0 \quad \text{where}$$

$$(2.37) \quad -\Delta S + \sigma F'(s^*)S = 0, \quad S|_{\Gamma} = 1.$$

Now we keep  $\sigma$  fixed but allow  $\Omega$  to vary in



$$(2.38) \quad \mathcal{Q}_Q^2 = \{\Omega \mid \Omega = T(Q), T \in \mathcal{L}^2\}$$

where  $Q$  is a given domain with  $C^2$  boundary and

$$(2.39) \quad \mathcal{L}^2 = \{T \mid T-I \text{ and } T^{-1}-I \in C_b^2(\mathbb{R}^n, \mathbb{R}^n)\}, \quad n = 2 \text{ or } 3.$$

Moreover, we impose the condition

$$(2.40) \quad \text{meas}(\Omega) = k.$$

Since the total quantity of enzyme in the membrane is proportional to  $\sigma \text{meas}(\Omega)$ , this quantity is constant when the shape of  $\Omega$  varies. We are interested in observing the influence of the shape of  $\Omega$  on the maximum activity  $a^*$ . This is not motivated by any direct industrial requirement, but is motivated by our desire to study the interaction of diffusion and reaction in simple artificial enzyme systems. We shall need the 2 formulas

$$(2.41) \quad \frac{\partial}{\partial \Omega} \left( \int_{\Omega} f_{\Omega} dx \right) \tau = \int_{\Omega} \frac{\partial f_{\Omega}}{\partial \Omega} \tau dx + \int_{\Gamma} f_{\Omega} \vec{n} \cdot \vec{\tau} d\Gamma$$

$$(2.42) \quad \frac{\partial}{\partial \Omega} \left( \int_{\Gamma} g_{\Omega} d\Gamma \right) \tau = \int_{\Gamma} \frac{\partial g_{\Omega}}{\partial \Omega} \tau d\Gamma + \int_{\Gamma} \left( \frac{\partial g_{\Omega}}{\partial n} + H g_{\Omega} \right) \vec{n} \cdot \vec{\tau} d\Gamma.$$

Here  $f_{\Omega}$  and  $g_{\Omega}$  are functions depending on the parameter  $\Omega$  and  $H$  is the mean curvature of the variety  $\partial\Omega = \Gamma$ .

Example  $f_{\Omega}(x) = 1 \quad \forall x \in \mathbb{R}^n$ ;  $\int_{\Omega} f_{\Omega} dx = \text{meas}(\Omega) \quad \frac{\partial f}{\partial \Omega} \Omega \tau = 0$   
 so that  $\frac{\partial}{\partial \Omega} (\text{meas} \Omega) = \int_{\Gamma} \vec{n} \cdot \vec{\tau} d\Gamma$ . If  $\text{meas}(\Omega) = k$ ,  $\int_{\Gamma} \vec{n} \cdot \vec{\tau} d\Gamma = 0$ . ■

Now we are able to calculate the differential of  $a^*(\Omega)$ :

$$A^* = \frac{\partial a^*}{\partial \Omega} \cdot \tau = \sigma \int_{\Omega} F'(s^*) S^* dx + \sigma \int_{\Gamma} F(s^*) \vec{n} \cdot \vec{\tau} d\Gamma$$

where  $S^* = \frac{\partial s^*}{\partial \Omega} \tau$ .

But on  $\Gamma$   $s^* = s_0^*$  so that  $\int_{\Gamma} F(s^*) \vec{n} \cdot \vec{\tau} d\Gamma = F(s_0^*) \int_{\Gamma} \vec{n} \cdot \vec{\tau} d\Gamma = 0$ .

Therefore

$$(2.43) \quad A^* = \sigma \int_{\Omega} F'(s^*) S^* dx.$$

$S^*$  satisfies the conditions obtained by differentiating equations (2.35):

$$(2.44) \quad -\Delta S^* + \sigma F'(s^*) S^* = 0 \quad \text{in } \Omega$$

$$(2.45) \quad S^* = S_0^* - \frac{\partial s^*}{\partial \nu} \vec{n} \cdot \vec{\tau} \quad \text{on } \Gamma.$$

The boundary condition (2.45) can be obtained by the following trick. Let  $\alpha$  be any function in  $C^\infty(\mathbb{R}^n)$ . Then

$$(2.46) \quad s^* = s_0^* \text{ on } \Gamma \Leftrightarrow \int_{\Gamma} (s^* - s_0^*) \alpha d\Gamma = 0 \quad \forall \alpha \in C^\infty(\mathbb{R}^n).$$

Apply (2.42):

$$\begin{aligned} \frac{\partial}{\partial n} \left( \int_{\Gamma} (s - s_0^*) \alpha d\Gamma \right) &= \int_{\Gamma} (S^* - S_0^*) \alpha d\Gamma \\ &+ \int_{\Gamma} \left[ \frac{\partial s^*}{\partial n} \alpha + (s^* - s_0^*) \frac{\partial \alpha}{\partial n} + H(s^* - s_0^*) \right] \vec{n} \cdot \vec{\tau} d\Gamma. \end{aligned}$$

As

$$s^* - s_0^* = 0 \text{ on } \Gamma$$

$$0 = \int_{\Gamma} (S^* - S_0^*) \alpha d\Gamma + \int_{\Gamma} \frac{\partial s^*}{\partial n} \alpha \vec{n} \cdot \vec{\tau} d\Gamma$$

whence (2.45). Now let us, at last, consider (2.36), (2.37), (2.43), (2.44) and (2.45), and introduce  $u = S^* - S_0^* S$ :

$$A^* = \sigma \int_{\Omega} F'(s^*) S^* dx = \int_{\Gamma} \frac{\partial S^*}{\partial n} d\Gamma = \int_{\Gamma} \frac{\partial S^*}{\partial n} d\Gamma - S_0^* \int_{\Gamma} \frac{\partial S}{\partial n} d\Gamma$$

or

$$(2.47) \quad A^* = \int_{\Gamma} \frac{\partial u}{\partial n} d\Gamma$$

and  $u$  satisfies

$$(2.48) \quad -\Delta u + \sigma F'(s^*) u = 0 \quad u|_{\Gamma} = - \frac{\partial s^*}{\partial n} \vec{n} \cdot \vec{\tau}.$$

In conclusion for a given  $\Omega$  the maximum activity



is obtained by solving (2.35), (2.36), (2.37), and the deformation of  $\Omega$  in order to increase this maximum activity (while  $\text{meas}(\Omega)$  and consequently the total quantity of enzyme remain fixed) is given by (2.47) and (2.48).

$$\left[ \frac{\partial^2 \Phi}{\partial x^2} + \frac{\partial^2 \Phi}{\partial y^2} + \frac{\partial^2 \Phi}{\partial z^2} \right] = 0$$

$$x^2 + y^2 + z^2 = 1$$

$$\left[ \frac{\partial^2 \Phi}{\partial x^2} + \frac{\partial^2 \Phi}{\partial y^2} + \frac{\partial^2 \Phi}{\partial z^2} \right] = 0$$

whence (2.42). Now for us, at first, consider (2.35), (2.37), (2.42), (2.44) and (2.45), and introduce  $u = s^* - s_0^*$ :

$$\left[ \frac{\partial^2 \Phi}{\partial x^2} + \frac{\partial^2 \Phi}{\partial y^2} + \frac{\partial^2 \Phi}{\partial z^2} \right] = 0$$

$$\left[ \frac{\partial^2 \Phi}{\partial x^2} + \frac{\partial^2 \Phi}{\partial y^2} + \frac{\partial^2 \Phi}{\partial z^2} \right] = 0$$

and  $u$  satisfies

$$\left[ \frac{\partial^2 \Phi}{\partial x^2} + \frac{\partial^2 \Phi}{\partial y^2} + \frac{\partial^2 \Phi}{\partial z^2} \right] = 0$$

In conclusion for a given  $\Omega$  the maximum activity

## CHAPTER III

Oscillations and Wave Front Propagation3.1. Oscillations: 0-dimensional case

One of the simplest situations in which oscillations arise is when a stable steady state loses its stability by undergoing a Hopf bifurcation. The steady state becomes unstable and gives rise to a branch of periodic solutions (Fig. 3.1).

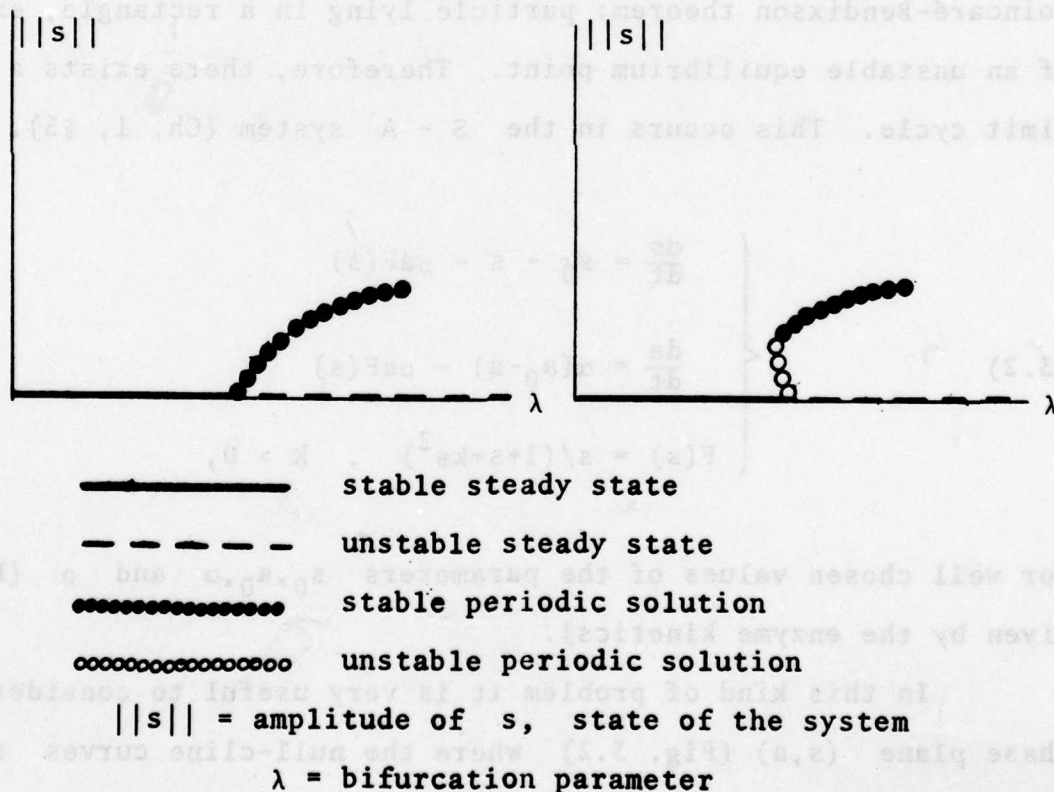


Figure 3.1

In particular if the system is governed by a pair of coupled ordinary differential equations

$$(3.1) \quad \begin{cases} \frac{ds}{dt} = f(s, a) \\ \frac{da}{dt} = g(s, a) \end{cases}$$

and if the "particle"  $(s(t), a(t))$  remains in a rectangle  $0 \leq s \leq s_0$ ,  $0 \leq a \leq a_0$ , then we satisfy the conditions of Poincaré-Bendixson theorem: particle lying in a rectangle, existence of an unstable equilibrium point. Therefore, there exists a stable limit cycle. This occurs in the S - A system (Ch. 1, §5).

$$(3.2) \quad \begin{cases} \frac{ds}{dt} = s_0 - s - \rho a F(s) \\ \frac{da}{dt} = \alpha(a_0 - a) - \rho a F(s) \\ F(s) = s/(1+s+ks^2) \quad , \quad k > 0, \end{cases}$$

for well chosen values of the parameters  $s_0, a_0, \alpha$  and  $\rho$  ( $k$  is given by the enzyme kinetics).

In this kind of problem it is very useful to consider the phase plane  $(s, a)$  (Fig. 3.2) where the null-cline curves  $f = 0$  and  $g = 0$



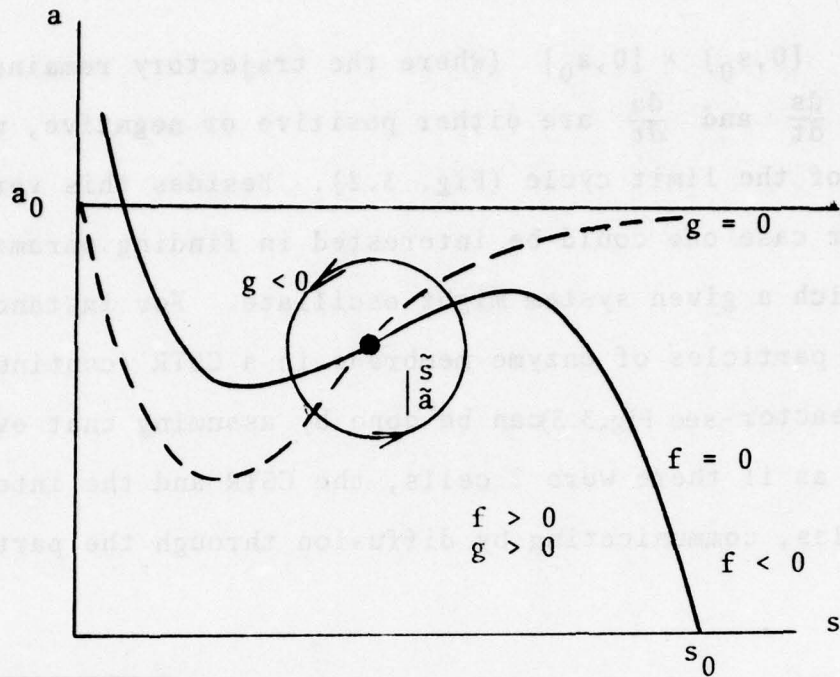


Figure 3.2

or

$$(3.3) \quad \begin{cases} s_0 - s - \rho a F(s) = 0 \\ \alpha(a_0 - a) - \rho a F(s) = 0 \end{cases}$$

separate the regions where  $f$  and  $g$ , hence  $\frac{ds}{dt}$  and  $\frac{da}{dt}$ , are positive or negative.

It is possible to find reasonable values of the parameters  $s_0, a_0, \rho, \alpha$  so that the null-clines have only one common point  $(\tilde{s}, \tilde{a})$ , an unstable equilibrium point of (3.2) Kernevez [20].

The isocline curves  $f = 0$  and  $g = 0$  separate the rec-

tangle  $[0, s_0] \times [0, a_0]$  (where the trajectory remains) in regions where  $\frac{ds}{dt}$  and  $\frac{da}{dt}$  are either positive or negative, whence the shape of the limit cycle (Fig. 3.2). Besides this very simple particular case one could be interested in finding parameter values for which a given system might oscillate. For instance, the modeling of particles of enzyme membrane in a CSTR (continuously stirred tank reactor-see Fig. 3.3) can be done by assuming that everything occurs as if there were 2 cells, the CSTR and the interior of the particles, communicating by diffusion through the particles. (Fig. 3.4)

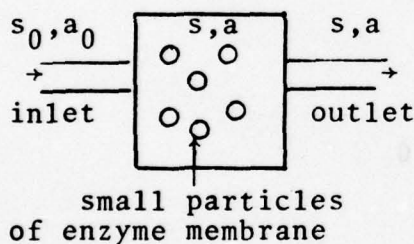


Figure 3.3

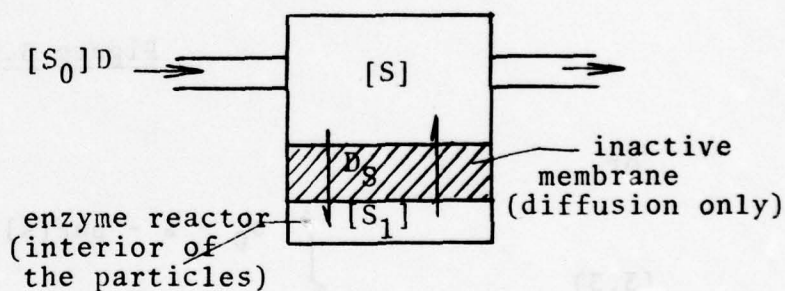


Figure 3.4

The model is

$$(3.4) \quad v \frac{d[S]}{dt} = D(S_0 - [S]) - D_S \frac{[S] - [S_1]}{L} .$$

Here  $V$  = CSTR volume,  $[S] = S$  concentration in CSTR,  $D$  = flow rate in CSTR,  $L$  (resp  $\sum$ ) = thickness (resp.area) of the membrane. Upon normilizing variables in (3.4), we obtain

$$(3.5) \quad \frac{ds}{dt} = \frac{1}{\theta}(s_0 - s) - \frac{1}{\theta}r(s - s_1).$$

Here  $s = [S]/K_S$ ,  $s_0 = [S_0]/K_S$ ,  $\theta = V/D$ ,  $\theta' = VL/(\sum D_S)$ . We have, similarly, for  $A$  in the CSTR:

$$(3.6) \quad \frac{da}{dt} = \frac{1}{\theta}(a_0 - a) - \frac{\beta}{\theta}r(a - a_1)$$

where  $\beta = \frac{D_A}{D_S}$ , where  $D_A$  is the diffusion coefficient in the membrane. In the cell corresponding to the enzyme membrane particles we have

$$v \frac{d[S_1]}{dt} = D_S \sum \frac{[S] - [S_1]}{L} - vr([S], [A]),$$

where  $v$  is the volume and  $r$  the rate of reaction, or

$$(3.7) \quad \frac{ds_1}{dt} = \frac{1}{\theta'_1}(s - s_1) - F(s_1, a_1)$$

where  $\theta'_1 = \frac{vL}{\sum D_S}$  and  $F(s_1, a_1) = \frac{r}{K_S}$ .

Similarly,

$$(3.8) \quad \frac{da_1}{dt} = \frac{1}{\theta'_1}(a - a_1) - F(s_1, a_1).$$



The result of this modelling is a set of four O.D.E.'s (3.5), (3.6), (3.7), and (3.8), including six parameters  $s_0, a_0, \theta, \theta', \theta'_1, \beta$ . The parameters  $\theta, \theta'$  and  $\theta'_1$  are characteristic times,  $\theta$  for the flow, the two others for diffusion. Now it is not evident that given the rate of reaction  $F(s, a)$  by a set of measurements (Fig. 3.5), we can choose the six parameters so that a stable periodic solution arises as a consequence of Hopf bifurcation. We shall have to use numerical analysis.

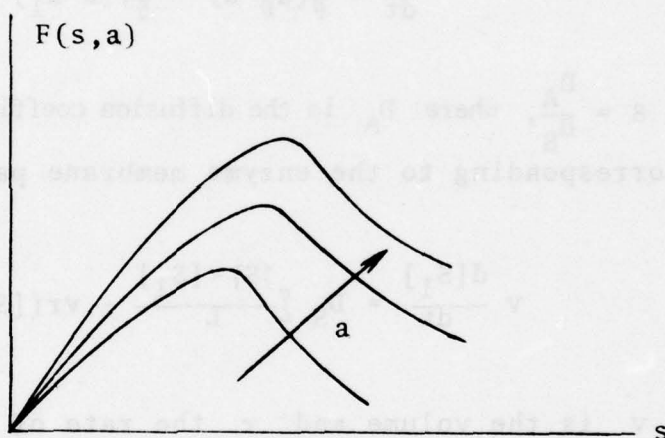


Figure 3.5

First, we identify the parameters  $\beta, \theta'$  and  $\theta'_1$  from experiments without reaction (that is with particles of membrane but without immobilized enzyme within them). Then, we explore all the possible steady states for the possibility of a Hopf bifurcation:

(i) Choose  $(\theta, s_1, a_1)$  and calculate  $s$  and  $a$  from (3.7) and (3.8) with  $\frac{ds_1}{dt} = \frac{da_1}{dt} = 0$ , and  $s_0$  and  $a_0$  from (3.5) and (3.6) with  $\frac{ds}{dt} = \frac{da}{dt} = 0$ .

(ii) Calculate the linearized operator of (3.5), (3.6), (3.7), (3.8)

$$(3.9) \quad \begin{bmatrix} -\frac{1}{\theta} - \frac{1}{\theta^r} & 0 & \frac{1}{\theta^r} & 0 \\ 0 & -\frac{1}{\theta} - \frac{\beta}{\theta^r} & 0 & \frac{\beta}{\theta^r} \\ \frac{1}{\theta_1} & 0 & -\frac{1}{\theta_1} - F_{s_1} & -F_{a_1} \\ 0 & \frac{1}{\theta_1} & -F_{s_1} & -\frac{1}{\theta_1} - F_{a_1} \end{bmatrix}$$

and calculate its eigenvalues.

If, all these eigenvalues being in the left half plane, it occurs that a pair of complex conjugate eigenvalues crosses the imaginary axis, then we can hope that a periodic solution will arise.

Now, we have to make this calculation for all the triples  $(\theta, s_1, a_1)$  in some region of  $\mathbb{R}^3$ . This is time consuming but it is practically impossible to experimentally find the desired

values of  $\theta, s_0$  and  $a_0$  for which the system oscillates.

### 3.2. Oscillations: 1-dimensional case

Equations (3.2) represent the interaction of diffusion ( $s_0-s$  and  $a_0-a$ ) and reaction ( $\sigma aF(s)$ ) in a system where these two phenomena take place in separated spatial regions. In the case of a distributed system such as an immobilized enzyme membrane, diffusion and reaction are governed by similar equations but in this case the diffusion terms  $s_0 - s$  and  $\alpha(a_0 - a)$  are replaced by  $\frac{\partial^2 s}{\partial x^2}$  and  $\alpha \frac{\partial^2 a}{\partial x^2}$ :

$$(3.9) \quad \left\{ \begin{array}{l} \frac{\partial s}{\partial t} - \frac{\partial^2 s}{\partial x^2} + \sigma aF(s) = 0 \\ \frac{\partial a}{\partial t} - \alpha \frac{\partial^2 a}{\partial x^2} + \sigma aF(s) = 0 \\ F(s) = s/(1+s+ks^2) \\ s(0,t) = s(1,t) = s_0, \quad a(0,t) = a(1,t) = a_0 \end{array} \right. \quad 0 < x < 1, t > 0$$

This system can oscillate. For instance, we choose  $s_0$  and  $a_0$  such that  $s_0 - \alpha a_0 = 0$ . Now if we look for steady state solutions of (3.9)

$$(3.10) \quad \left\{ \begin{array}{l} - \frac{d^2 s}{dx^2} + \sigma aF(s) = 0 \\ - \alpha \frac{d^2 a}{dx^2} + \sigma aF(s) = 0 \end{array} \right. \quad \begin{array}{l} s(0) = s(1) = s_0 \\ a(0) = a(1) = a_0, \end{array}$$



we see that  $u = s - \alpha a$  satisfies

$$(3.11) \quad -\frac{d^2 u}{dx^2} = 0, \quad u(0) = 0, \quad u(1) = 0$$

so that  $u \equiv 0$ ,  $a = \frac{1}{\alpha} s$ , and

$$(3.12) \quad -s'' + \frac{\sigma}{\alpha} \frac{s^2}{1+s+ks^2} = 0, \quad s(0) = s(1) = s_0.$$

This latter equation admits one solution  $\tilde{s}$  since  $s \rightarrow \frac{s^2}{1+s+ks^2}$  is monotone. The corresponding steady state for (3.9),  $s = \tilde{s}(x)$ ,  $a = \tilde{a}(x)$ , can be analyzed for stability by calculating the eigenvalues of the linearized operator

$$\begin{bmatrix} u \\ v \end{bmatrix} \rightarrow \begin{bmatrix} -u'' + \sigma \tilde{a}(x) F'(\tilde{s}(x)) u + \sigma F(\tilde{s}(x)) v \\ -\alpha v'' + \text{---} \end{bmatrix}$$

The pair of complex conjugate leading eigenvalues behaves, when  $\sigma$  varies, as depicted in Figure 3.6.

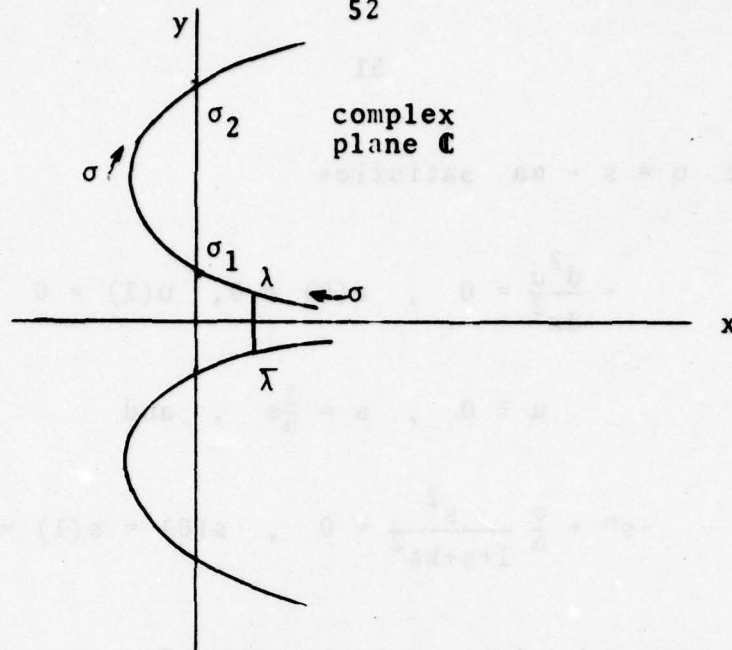
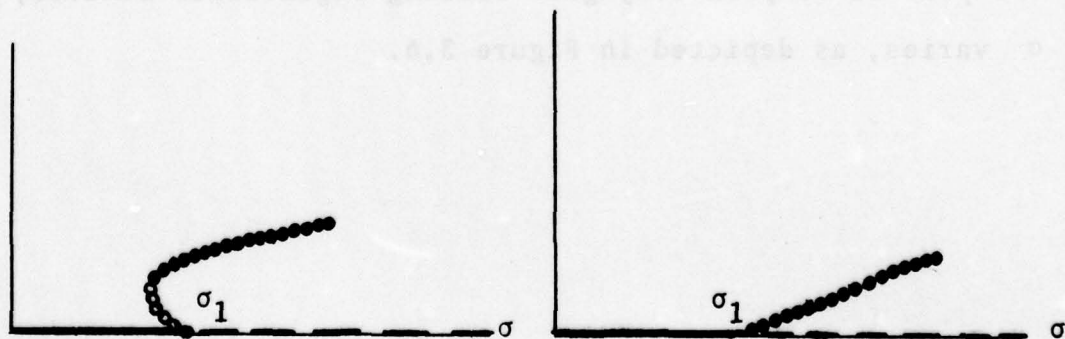


**Figure 3.6**  
Plot of the two leading eigenvalues  $\lambda$  and  $\bar{\lambda}$  when  $\sigma$  varies.

We see that when  $\sigma$  enters into the interval  $(\sigma_1, \sigma_2)$ , the state  $(\tilde{s}, \tilde{a})$  loses its stability and a family of periodic solutions arise by Hopf bifurcation. There are two possibilities (Figure 3.7).



subcritical bifurcation

supercritical bifurcation

**Figure 3.7**

From a numerical point of view, if we solve the equations (3.9) for  $\sigma$  slightly larger than  $\sigma_1$ , we find a periodic oscillation of the  $s$  and  $a$  profiles of concentration, but we cannot decide whether the bifurcation is sub- or super-critical. Further calculations would be necessary to check that.

### 3.3. Wave front propagation

We consider here the  $S - A$  system equations (Ch.I, §5)

$$(3.13) \quad \begin{cases} \frac{\partial s}{\partial t} - \frac{\partial^2 s}{\partial x^2} + \gamma[F(s,a) - (s_0 - s)] = 0 & 0 < x < 1, \quad t > 0, \\ \frac{\partial a}{\partial t} - \beta \frac{\partial^2 a}{\partial x^2} + \gamma[F(s,a) - \alpha(a_0 - a)] = 0 \\ F(s,a) = \rho a s / (1 + s + k s^2) \\ \frac{\partial s}{\partial x} = \frac{\partial a}{\partial x} = 0 \quad \text{at } x = 0 \quad \text{and } x = 1. \end{cases}$$

We suppose that, in the  $(s,a)$  plane, the null-clines

$$(3.14) \quad \begin{cases} f(s,a) = F(s,a) - (s_0 - s) = 0 \\ g(s,a) = F(s,a) - \alpha(a_0 - a) = 0 \end{cases}$$

are as indicated in Figure 3.8.



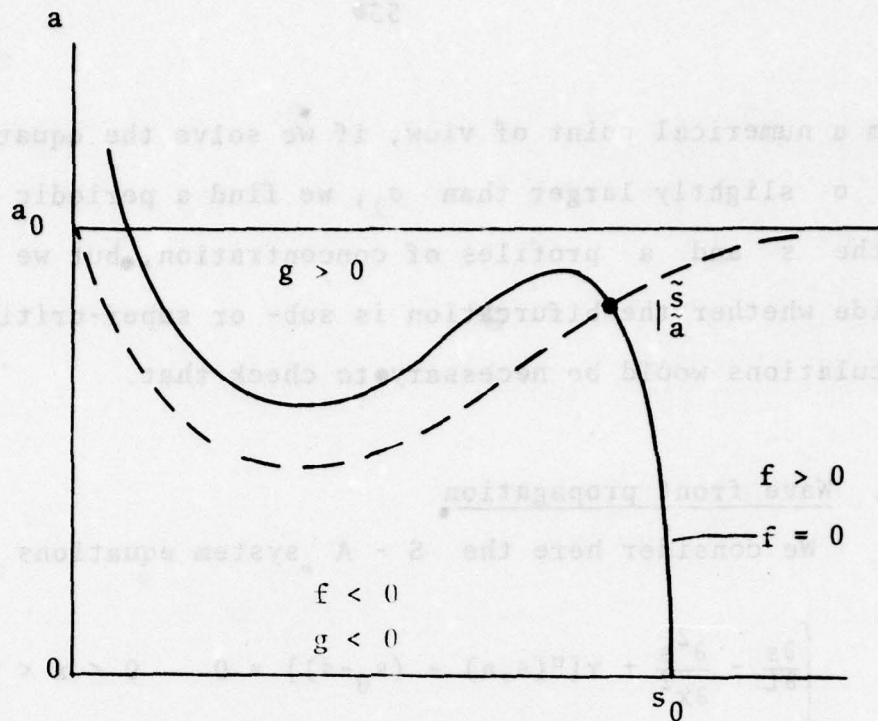


Figure 3.8

They possess only one common point  $(\tilde{s}, \tilde{a})$ , which is situated near the top of the curve  $f = 0$ , and which is stable for the dynamical system

$$(3.15) \quad \begin{cases} \frac{ds}{dt} + f(s, a) = 0 \\ \frac{da}{dt} + g(s, a) = 0. \end{cases}$$

In order to understand the behavior of the distributed system (3.13), let us first describe the trajectory of a particle subject to (3.15) when it starts from  $P_0$  (Fig. 3.9).

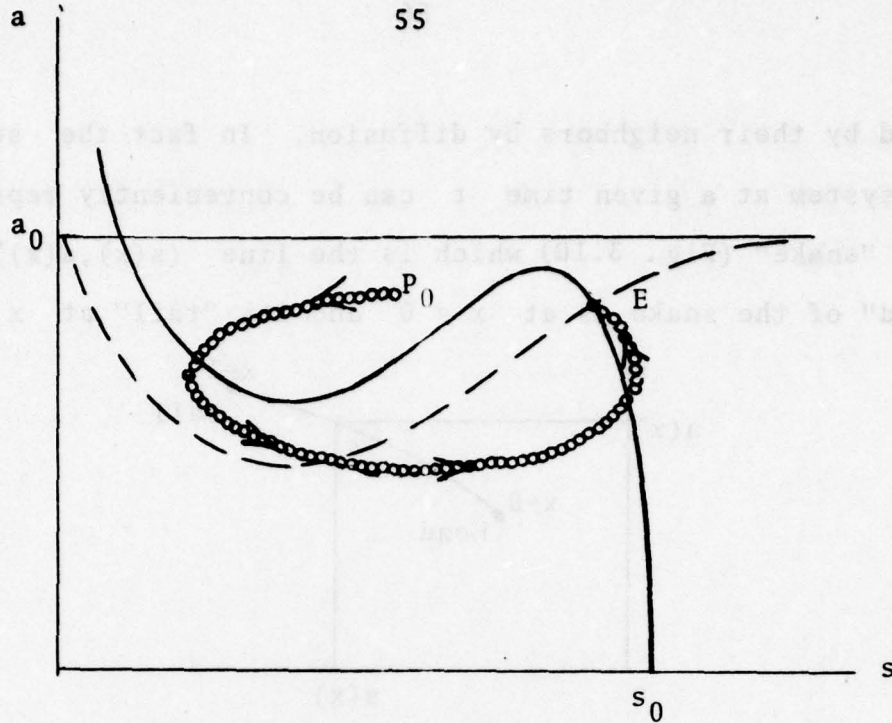


Figure 3.9

Due to the sign of  $\frac{ds}{dt}$  and  $\frac{da}{dt}$  in (3.15), in the regions delineated by the isoclines, this trajectory is as shown in Figure 3.9: going South-West in a first phase (fast phase), going South-East in a second phase (slow phase), North-East in a fast third phase and North-West towards the equilibrium point E in a last phase which is slow. The fact that some phases are fast and others slow is due to the respective order of magnitude of  $f$  and  $g$  in these phases of the movement.

Now in the case of the distributed dynamical system (3.13), instead of one particle we have a continuum of them, each one corresponding to a value of  $x$ ,  $0 < x < 1$ . In addition to the dynamics due to the terms  $f$  and  $g$ , these particles are influ-

enced by their neighbors by diffusion. In fact the state of the system at a given time  $t$  can be conveniently represented by a "snake" (Fig. 3.10) which is the line  $(s(x), a(x))_{0 < x < 1}$ . The "head" of the snake is at  $x = 0$  and its "tail" at  $x = 1$ .

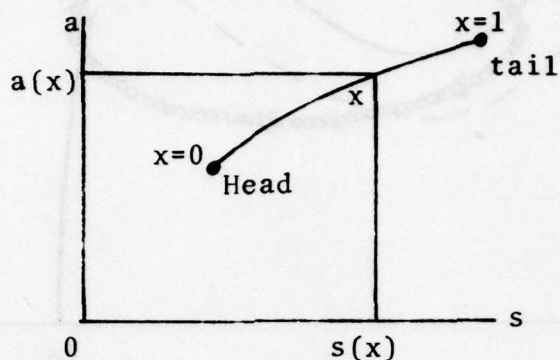


Figure 3.10

Let us start with the system (3.13) at the (diffusionally stable) steady state  $(\tilde{s}, \tilde{a})$ . The "snake" is concentrated into the point  $(\tilde{s}, \tilde{a})$  and the  $S$  and  $A$  profiles are as shown in Figure 3.11 a) and b). Then, during some time interval  $(0, \tau)$ , we suppose that  $s_0$ , instead of having a constant value  $\tilde{s}_0$ , is perturbed near  $x = 0$  (Figure 3.11 c)). The consequence is to modify the profiles of  $S$  and  $A$ , mainly that of  $S$ , together with the shape of the snake in the phase plane (Figure 3.12).

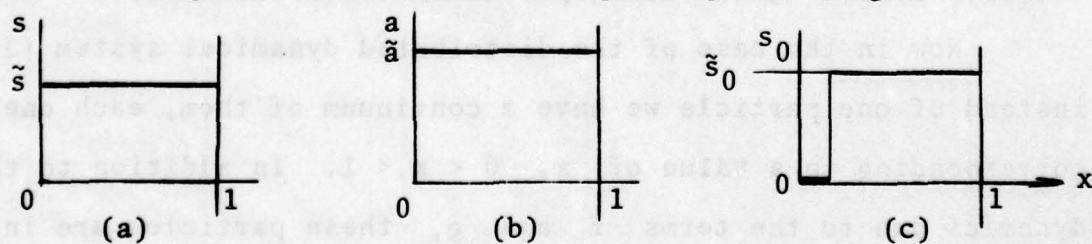


Figure 3.11



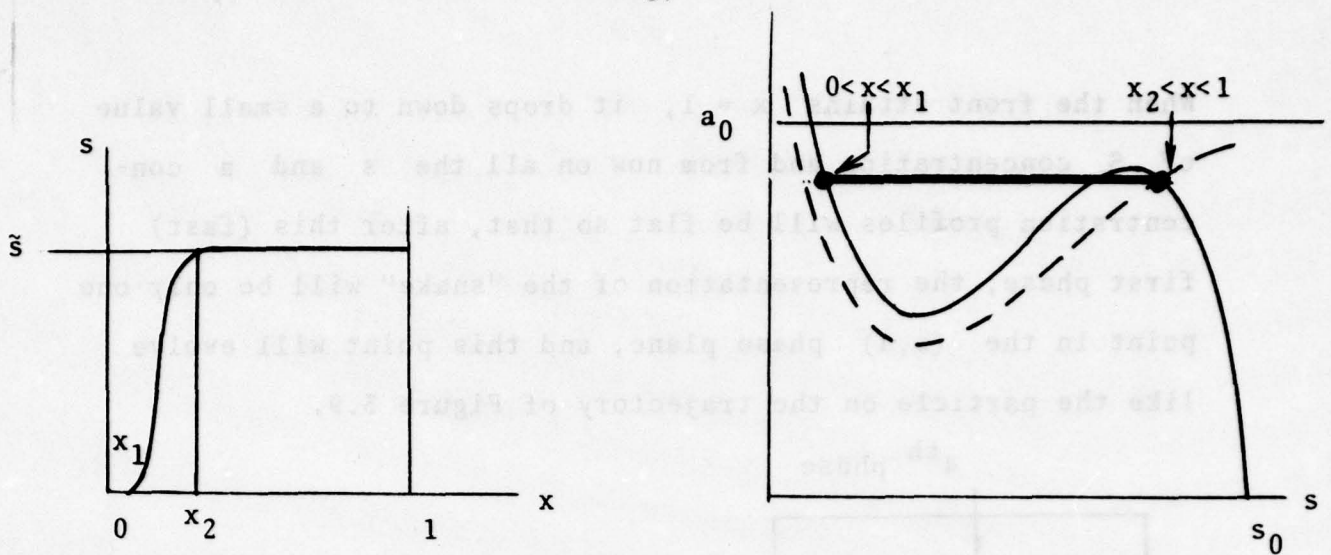


Figure 3.12

After the  $S$  profile has been so perturbed, we can restore  $s_0$  to a uniform value  $\tilde{s}_0$  for  $0 < x < 1$ , the front of  $S$  concentration between  $x_1$  and  $x_2$  is going to propagate rapidly towards  $x = 1$  (Figure 3.13).

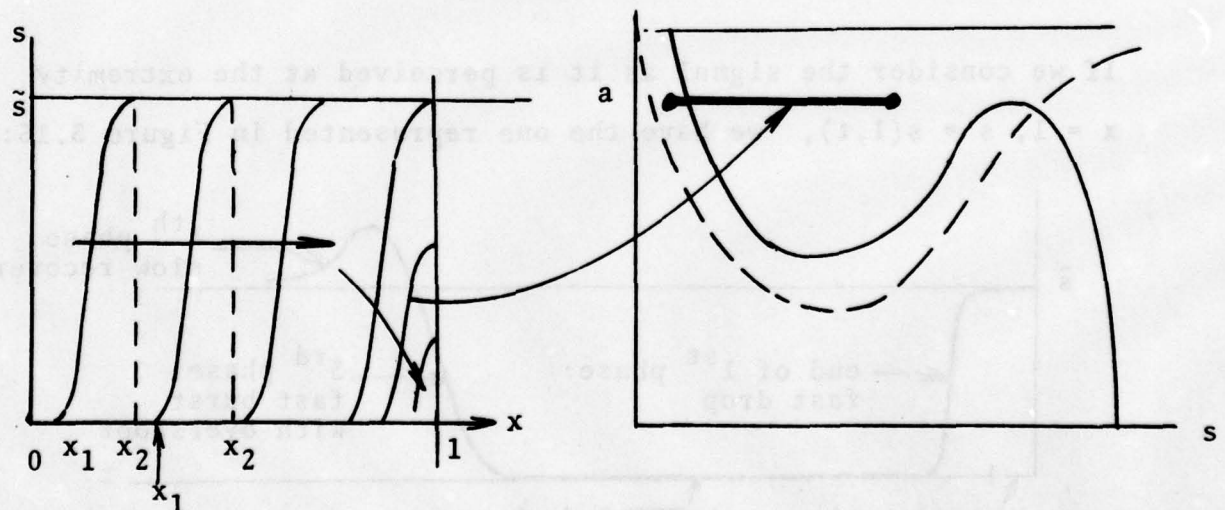


Figure 3.13

When the front attains  $x = 1$ , it drops down to a small value of  $S$  concentration and from now on all the  $s$  and  $a$  concentration profiles will be flat so that, after this (fast) first phase, the representation of the "snake" will be only one point in the  $(s,a)$  phase plane, and this point will evolve like the particle on the trajectory of Figure 3.9.

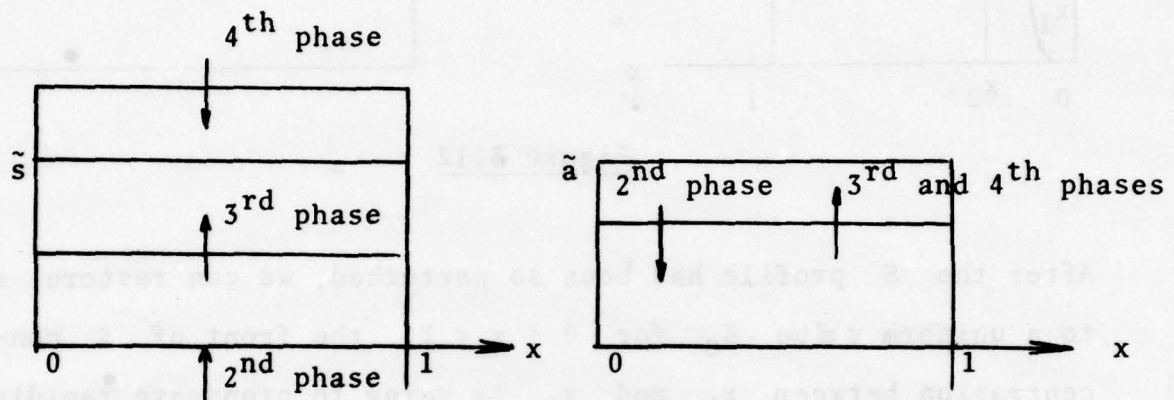


Figure 3.14

If we consider the signal as it is perceived at the extremity  $x = 1$ ,  $s = s(1,t)$ , we have the one represented in Figure 3.15:

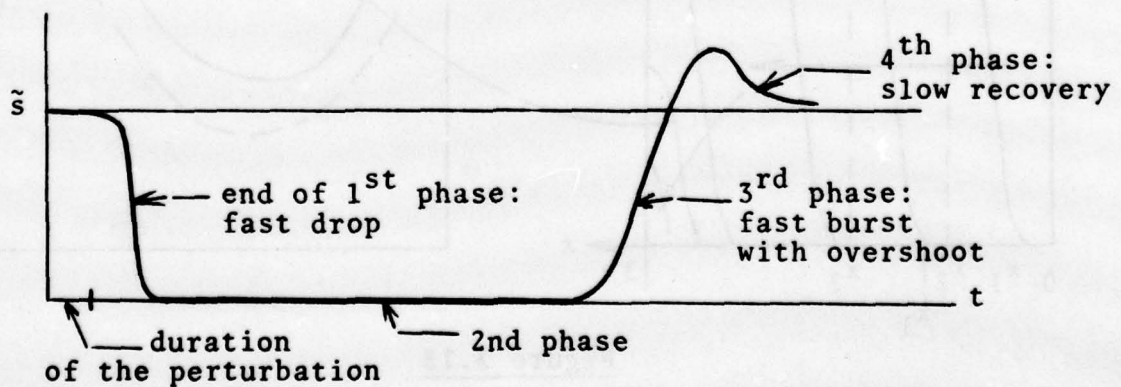


Figure 3.15

In a system similar to (3.13), but with no reaction, a similar perturbation would not be propagated.

#### Pattern formation 4.1. Introduction

Morphogenesis in insects is one of the best-known phenomena of pattern formation in biology. This is due to the fact that Drosophila flies, for example, have been extensively studied for several decades by many biologists. They have observed the following parts of the adult epidermis, such as a wing, a leg, a haltere, the eye-antenna part or the genital part, are formed of cells which are differentiated at the beginning of the development were undifferentiated within what is called an imaginal disk. In fact in early stages of development an imaginal disk is formed of very few cells, say 40. Marker experiments show that even at the beginning all the cells of a given imaginal disk have the same potentialities, after some time there is a difference between their components. Take the wing disc, for example. Cells first differentiate between those which will give the anterior part of the wing, and those which will give the posterior part. This can be seen by marking a cell after that differentiation: her daughters will remain in the same compartment. If the cell had been marked before the creation of a boundary, her daughters would have been able to go in any place of the imaginal disk, and her descendants could have been observed in any of the compartments which form later. So a cell marked just after the creation of the anterior and posterior compartments will have daughters only in the same



## CHAPTER IV

Pattern Formation4.1. Introduction

Morphogenesis in insects is one of the best-known phenomena of pattern formation in embryos. This is due to the fact that *Drosophila* flies, for example, have been extensively studied for several decades by many zoologists. They have observed the following: parts of the adult epidermis, such as a wing, a leg, a haltere, the eye-antenna part or the genital part, are formed of cells which are differentiated but at the beginning of the development were undifferentiated within what is called an imaginal disk. In fact in early stages of development an imaginal disk is formed of very few cells, say 40. Marker experiments show that even if at the beginning all the cells of a given imaginal disk have the same potentialities, after some time there is a difference between their commitments. Take the wing disc, for example. Cells first differentiate between those which will give the anterior part of the wing, and those which will give the posterior part. This can be seen by marking a cell after that differentiation: her daughters will remain in the same compartment. If the cell had been marked before the creation of a boundary, her daughters would have been able to go in any place of the imaginal disc, and her descendants could have been observed in any of the compartments which form later. So a cell marked just after the creation of the anterior and posterior compartments will have daughters only in the same

compartment as itself, but everywhere in this compartment. Subsequent separations form: dorsal-ventral, wing-thorax,... . At each compartment formation something induces a different commitment to the cells (and their daughters) according to whether they are in one part or another of the spatial domain. Kauffman et al [18] suggested that the cause could be chemical patterns of concentrations in a 2-species diffusion-reaction system:

$$(4.1) \quad \begin{cases} \frac{\partial s}{\partial t} - \Delta s + f(s, a; \gamma) = 0 \\ \frac{\partial a}{\partial t} - \beta \Delta a + g(s, a; \gamma) = 0 \\ \frac{\partial s}{\partial n} = 0 \quad \frac{\partial a}{\partial n} = 0 \end{cases} \quad \begin{array}{l} \text{in } \Omega \\ \\ \text{on } \Gamma = \partial\Omega. \end{array}$$

Here  $\Omega$  is the imaginal disc and  $\gamma$  is a parameter. Depending on the values of  $\gamma$ , the system (4.1) possesses various stable non-uniform steady state (N.U.S.S.) solutions. When such a solution arises, those cells where  $s$ , for example, is above some threshold concentration, will differentiate in some way, the others in the alternate way.

The chemical basis of morphogenesis had already been suggested by Turing [19] in what is more and more considered as a pioneering paper. Later on Prigogine and his group [2] pointed out that self-organization could result from the inter-

action of diffusion and reaction in dissipative structures.

On the other hand artificial enzyme membranes (Thomas et al [8]) are a good tool to study, in a well-defined context, basic phenomena occurring in living systems: enzymes are catalysts of most biochemical reactions, and in living media they are, in general, immobilized among other protein molecules in structures where diffusion, in addition to reaction, play a role. By linking enzyme molecules to inactive protein molecules, Thomas and coworkers prepare artificial enzyme membranes in which it is possible to obtain hysteresis, oscillations, pattern formation and wave front propagation. (Kernevez et al, [20, 21]). The fact that pattern formation can occur in so simple a context and in a structure which is likely to occur in many biological situations adds support to Kauffman's theory.

The so-called S - A system models the situation of an active layer separated from an external reservoir by an inactive layer (Figure 4.1).

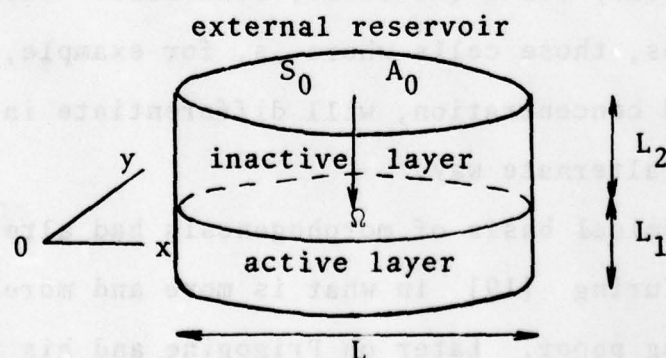


Figure 4.1



The modelling assumes that in the active layer the concentrations of S and A depend only on x and y, coordinates in the plane of  $\Omega$ , and that the fluxes of S and A coming from the reservoir to the active layer through the inactive layer are simply proportional to the differences of concentrations  $S_0 - [S]$  and  $A_0 - [A]$  where  $S_0$  and  $A_0$  are concentrations in the reservoir. Within the active layer 3 phenomena occur: diffusion in the directions of the plane of  $\Omega$ , with coefficients  $D_S$  and  $D_A$ , S inhibited and A activated reaction, with rate

$$(4.2) \quad r = V_M \frac{[A]}{K_A} \frac{[S]}{K_S + [S] (1 + \frac{[S]}{K_{SS}})},$$

and feeding from outside with fluxes

$$(4.3) \quad J_S = D'_S \frac{S_0 - [S]}{L_2} \quad \text{and} \quad J_A = D'_A \frac{A_0 - [A]}{L_2}.$$

The coefficients in (4.2) are, respectively,

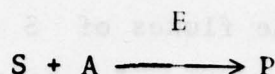
$V_M$  = constant, proportional to the enzyme concentration

$K_A$  = Michaelis constant of the enzyme for A

$K_S$  = Michaelis constant of the enzyme for S

$K_{SS}$  = inhibition constant.

An example of such a reaction is



where E is the enzyme uricase, S is uric acid, A is oxygen, and P allantoin plus other products.

The balance of masses for S in an elementary volume of active layer gives (Figure 4.2)

$$L_1(d\Omega) \frac{\partial[S]}{\partial t'} = L_1(d\Omega) D_S \left( \frac{\partial^2[S]}{\partial x'^2} + \frac{\partial^2[S]}{\partial y'^2} \right)$$

$$-L_1(d\Omega) v_M \frac{[A]}{K_S} \frac{[S]}{K_S + [S] (1 + \frac{[S]}{K_{SS}})} + D'_S(d\Omega) \frac{S_0 - [S]}{L_2},$$

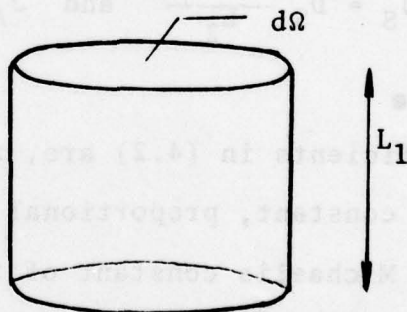


Figure 4.2

whence we obtain, by taking as new units  $K_S$  for concentrations,

$L$  (i.e., some characteristic length of  $\Omega$ , for example, its diameter) for length,  $\theta = L^2/D_S$  for time, and dividing by  $L_1(d\Omega)K_S/\theta$ :

$$(4.4) \quad \frac{\partial s}{\partial t} - \Delta s + \gamma[F(s, a) - (s_0 - s)] = 0.$$

Here  $s = [S]/K_S$ ,  $a = [A]/K_S$ ,  $t = t'/\theta$ ,  $\Delta$  denotes  $\frac{\partial^2}{\partial x^2} + \frac{\partial^2}{\partial y^2}$ ,  $x$  and  $y$  new coordinates with  $L$  as unit:  $x = x'/L$ ,  $y = y'/L$ ,  $\gamma = \frac{D'_S}{L_1 L_2} \theta = \frac{\theta}{\theta'}$  if  $\theta' = \frac{L_1 L_2}{D_S}$ .

$$(4.5) \quad F(s, a) = \rho a \frac{s}{1+s+ks^2}$$

$$\rho = (V_M/K_A)\theta', \quad k = \frac{K_S}{K_{SS}}.$$

Similarly we have for  $A$

$$(4.6) \quad \frac{\partial a}{\partial t} - \beta \Delta a + \gamma[F(s, a) - \alpha(a_0 - a)] = 0$$

$$\alpha = D'_A/D'_S, \quad \beta = D_A/D_S.$$

Finally, we have no-flux boundary conditions on  $\Gamma = \partial\Omega$ :

$$(4.7) \quad \frac{\partial s}{\partial n} = 0, \quad \frac{\partial a}{\partial n} = 0 \quad \text{on } \Gamma$$



where  $\partial/\partial n$  is, say, the outward normal derivative. Summing up, the S - A system is governed by

$$(4.8) \quad \left\{ \begin{array}{l} \frac{\partial s}{\partial t} - \Delta s + \gamma[F(s,a) - (s_0 - s)] = 0 \\ \frac{\partial a}{\partial t} - \beta \Delta a + \gamma[F(s,a) - \alpha(a_0 - a)] = 0 \\ F(s,a) = \rho a s / (1 + s + k s^2) \\ \frac{\partial s}{\partial n} = 0, \quad \frac{\partial a}{\partial n} = 0. \end{array} \right.$$

We shall use the notation

$$\begin{aligned} f(s,a) &= F(s,a) - (s_0 - s) \\ g(s,a) &= F(s,a) - \alpha(a_0 - a) \end{aligned}$$

in the following discussions.

Let us point out the fact that all the parameters are without dimension:  $s_0$  and  $a_0$ , representing concentrations in the environment;  $\rho$  which is the ratio between 2 times;  $\theta'$ , characterizing the access of substrates from the outside to the active layer through the inactive layer;  $\frac{K_A}{V_M}$ , characteristic time of the enzyme reaction;  $\alpha$  and  $\beta$ , ratios of diffusion coefficients;  $k$ , ratio of concentrations; and  $\gamma$ , ratio of  $\theta$  and  $\theta'$ , characteristic times of diffusion within the active layer and of transport to the active layer.

In applications only  $k$  and  $\beta$  are imposed:  $k$  of the order of 0.1 or 1,  $\beta$  of the order of 5. The other parameters,  $s_0, a_0, \alpha, \rho$  and  $\gamma$ , are at our disposal.

It can be shown (Kernevez [20]) that these parameters can be chosen in such a way that the so-called isocline curves  $f(s,a) = 0$  and  $g(s,a) = 0$  (Figure 4.3) have only one common point  $(\tilde{s}, \tilde{a})$ , a stable steady state (node) of the dynamical system

$$(4.9) \quad \frac{ds}{dt} + f(s,a) = 0 \quad \frac{da}{dt} + g(s,a) = 0$$

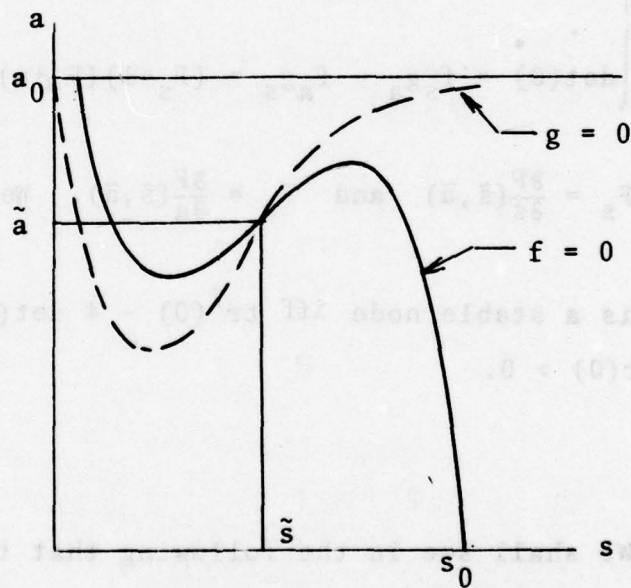


Figure 4.3: isoclines in the phase plane

Equivalently, the nature of the steady state  $(\tilde{s}, \tilde{a})$  for (4.9)

can be expressed by saying that  $\lambda_1 > 0$  and  $\lambda_2 > 0$ ,  $\lambda_1$  and  $\lambda_2$  being the eigenvalues of the linearized operator

$$\begin{bmatrix} f_s & f_a \\ g_s & g_a \end{bmatrix}$$

around  $(\tilde{s}, \tilde{a})$ . Let us call

$$(4.10) \quad \begin{cases} \text{tr}(0) = f_s + g_a = F_s + 1 + F_a + \alpha \\ \det(0) = f_s g_a - f_a g_s = (F_s + 1)(F_a + \alpha) - F_s F_a = \alpha F_s + F_a + \alpha \end{cases}$$

where  $F_s = \frac{\partial F}{\partial s}(\tilde{s}, \tilde{a})$  and  $F_a = \frac{\partial F}{\partial a}(\tilde{s}, \tilde{a})$ . We have that

$(\tilde{s}, \tilde{a})$  is a stable node iff  $\text{tr}^2(0) - 4 \det(0) > 0$ ,  $\det(0) > 0$ , and  $\text{tr}(0) > 0$ .

We shall see in the following that the first inequality will be a consequence of others. Therefore we only require the following conditions

$$(4.11) \quad \begin{cases} \text{tr}(0) = F_s + 1 + F_a + \alpha > 0 \\ \det(0) = \alpha F_s + F_a + \alpha > 0 \end{cases}$$



Now one can observe that  $(\tilde{s}, \tilde{a})$  is a trivial solution not only of (4.9) but also of (4.8). This is due to the fact that  $s(x, y, t) \equiv \tilde{s}$ ,  $a(x, y, t) \equiv \tilde{a}$ , profiles of concentration constant in time and spatially uniform, satisfy  $\frac{\partial s}{\partial t} = 0$ ,  $\frac{\partial a}{\partial t} = 0$ ,  $-\Delta s = 0$ ,  $-\Delta a = 0$ ,  $f(s, a) = 0$ ,  $g(s, a) = 0$ ,  $\frac{\partial s}{\partial n} = 0$  and  $\frac{\partial a}{\partial n} = 0$ .

As  $(\tilde{s}, \tilde{a})$  is stable for (4.9), one can ask if  $(\tilde{s}, \tilde{a})$  is still stable for (4.8). All the parameters being fixed, except  $\gamma$ , we shall see that the answer is yes, if  $\gamma$  is small enough, and no, if  $\gamma$  is large enough. ( $\gamma$  small means  $\theta$  small with respect to  $\theta'$ , i.e., diffusion of  $S$  within the active layer fast in comparison with the transport of  $S$  from the outside to the active layer). In fact, the situation is more complex since, as we shall see, when  $\gamma$  is increasing,  $(\tilde{s}, \tilde{a})$  can lose its stability, then recover it, and this can occur several times, before the point finally becomes and remains unstable.

Finally, let us suppose that in the following all the parameters, except  $\gamma$ , will be kept fixed.  $\gamma$  will be the bifurcation parameter. Let us recall that  $\gamma = \frac{L^2}{D_S} \theta'$ , so that if  $D_S$  and  $\theta'$  are kept fixed,  $\gamma$  is proportional to  $\text{meas}(\Omega)$ . Therefore, one can view (4.8) as the modelling of an expanding disc (like an imaginal disc) after normalization of the spatial domain to a domain  $\Omega$  with diameter 1, the size of the disc being determined by the coefficient  $\gamma$ . If the size of the spatial domain does not vary,  $\gamma$  may change for other reasons, for example, because  $\theta'$  increases, and since  $\theta' = L_1 L_2 / D_S'$ , this can be due to a decrease of  $D_S'$ .

## 4.2. Linear stability analysis

Let us make the change of variables

$$s = \tilde{s} + u, \quad a = \tilde{a} + v$$

and denote

$$U = [u, v]^T$$

Equations (4.8) can be written

$$(4.12) \quad \frac{dU}{dt} + (L_0 + \gamma L_1)U + \gamma M(U) = 0$$

where

$$(4.13) \quad L_0 = \begin{bmatrix} -\Delta & 0 \\ 0 & -\beta\Delta \end{bmatrix}, \quad L_1 = \begin{bmatrix} F_s + 1 & F_a \\ F_s & F_a + \alpha \end{bmatrix}$$

$$(4.14) \quad M(U) = N(U) \begin{bmatrix} 1 \\ 1 \end{bmatrix}, \quad N(U) = F(\tilde{s} + u, \tilde{a} + v) - F(\tilde{s}, \tilde{a}) - F_s u - F_a v$$

$$(N(U) = O(u^2 + v^2)).$$

It can be shown (Meurant and Saut [26]) that the operators  $L_\gamma = L_0 + \gamma L_1$  and  $M_\gamma = \gamma M$  possess a number of desirable properties such as:

Lemma 4.1. For all  $\gamma \in \mathbb{R}^+$

- (i)  $L_\gamma$  is a closed linear operator with domain  $\mathcal{D} = \{(u, v) \in H^2(\Omega)^2, \frac{\partial u}{\partial n} = 0, \frac{\partial v}{\partial n} = 0\}$  in  $H = L^2(\Omega)^2$ .
- (ii)  $L_\gamma$  is  $m$ -sectorial with half angle  $\pi/4$ .
- (iii) The resolvent of  $L_\gamma$  is compact (the spectrum of  $L_\gamma$  is therefore discrete and only composed of eigenvalues having a finite multiplicity).
- (iv)  $L_\gamma$  is the infinitesimal generator of an analytic semigroup  $e^{-L_\gamma t}$  which satisfies

$$\|e^{-L_\gamma t}\|_{\mathcal{L}(K, D)} \leq \frac{c}{t^{1/2}}, \quad t \in ]0, T[, \quad c > 0,$$

where  $K = H^1(\Omega)^2$ .

- (v)  $\{L_\gamma\}$  is a holomorphic family of type (A).

Lemma 4.2.

- (i)  $M_\gamma : \mathcal{D} \rightarrow K$  is analytic
- (ii)  $\|M_\gamma(0)\|_K \leq C \|U\|_\phi^2$

The reason we give these properties is that when they are satisfied and when  $\gamma_0$  is such that the spectrum of  $L_{\gamma_0}$  crosses the imaginary axis by the simple eigenvalue 0, the remaining part of the spectrum lying in the half space  $\operatorname{Re}(z) > 0$ , then we have:



Theorem 4.1. There exists in  $\mathcal{D}$  a solution  $U(\gamma) = [u(\gamma), v(\gamma)]^T \neq [0,0]^T$  of  $L_\gamma U + M_\gamma(U) = 0$  which is defined in a neighborhood of  $\gamma_0$ . Moreover, if the bifurcation is bilateral ( $U(\gamma)$  defined on the left and right sides of  $\gamma_0$ ),  $U(\gamma)$  is analytic in  $\gamma$ , and if the bifurcation is one-sided,  $U(\gamma)$  is analytic in  $|\gamma - \gamma_0|^{1/2}$ . If the bifurcation is bilateral, there is "exchange of stabilities". If the bifurcation is one-sided  $U(\gamma)$  is stable or not according to whether it is on the side where the trivial steady state is unstable.

From a practical viewpoint, we must now effectively study the eigenvalues of  $L_\gamma$ , to see whether we are in the case where Theorem 4.1 is applicable; this will be the subject of this paragraph. We then shall have to elucidate the nature of the bifurcation (bilateral or one sided, on which side); this will be done in §3 by a modified perturbation analysis.

Now the problem is: we know that  $U = 0$  is stable or not according to whether the spectrum of  $L_\gamma$  lies in  $\text{Re}(z) > 0$  or at least one of its eigenvalues lies in  $\text{Re}(z) < 0$ . So we are seeking  $\lambda$  and  $\phi$  such that (the eigenvalue problem)

$$(4.15) \quad L_\gamma \phi = \lambda \phi.$$

We can look for  $\phi$  in the form

$$(4.16) \quad \phi_n = \begin{bmatrix} 1 \\ M_n \end{bmatrix} w_n$$

where  $w_n$  is the  $n^{\text{th}}$  eigenfunction of  $-\Delta$  on  $\Omega$  subject to no-flux boundary conditions:

$$(4.17) \quad -\Delta w_n = \mu_n w_n, \quad \frac{\partial w_n}{\partial n} = 0, \quad \int_{\Omega} w_n^2 d\Omega = 1.$$

Substituting (4.16) into (4.15), we obtain

$$(4.18) \quad \begin{bmatrix} \mu_n + \gamma(F_s + 1) - \lambda & \gamma F_a \\ \gamma F_s & \beta \mu_n + \gamma(F_a + \alpha) \end{bmatrix} \begin{bmatrix} 1 \\ M_n \end{bmatrix} = \begin{bmatrix} 0 \\ 0 \end{bmatrix}.$$

This admits a solution iff the determinant of the matrix in (4.18) is null, that is

$$(4.19) \quad \lambda^2 - \text{tr}(n)\lambda + \det(n) = 0.$$

Here

$$(4.20) \quad \begin{cases} \text{tr}(n) = (\beta+1)\mu_n + \gamma(F_s+1+F_a+\alpha) \\ \det(n) = \gamma^2 T\left(\frac{\mu_n}{\gamma}\right) \quad \text{where} \\ T(z) = \beta z^2 + (\beta(F_s+1)+F_a+\alpha)z + \alpha F_s + F_a + \alpha. \end{cases}$$

Therefore, to each eigenvalue  $\mu_n$  of  $-\Delta$  ( $n=0,1,2,\dots$ ), there will correspond 2 eigenvalues of  $L_\gamma$ ,  $\lambda_n^-$  and  $\lambda_n^+$ , solutions of (4.19), and to each one will be associated a value  $M_n^\pm$  by

$$(4.21) \quad \mu_n + \gamma(F_s+1) - \lambda_n^\pm + \gamma F_a M_n^\pm = 0$$

thus determining the corresponding eigenvector  $\phi_n^\pm$ :

$$(4.22) \quad \phi_n^\pm = \begin{bmatrix} 1 \\ M_n^\pm \end{bmatrix} w_n.$$

**Proposition 4.1.** Under the assumptions

$$(4.23) \quad F_s < 0, \quad \alpha > 1, \quad \beta > 1$$

then the solutions  $\lambda_n^\pm$  of (4.19) are real numbers ( $\lambda_n^- < \lambda_n^+$ ).

**Proof.**  $\Delta(n) = \text{tr}^2(n) - 4\det(n)$

$$= [(\beta-1)\mu_n + \gamma((F_a^{1/2} - (-F_s)^{1/2})^2 + \alpha - 1)][(\beta-1)\mu_n + \gamma((F_a^{1/2} + (-F_s)^{1/2})^2 + \alpha - 1)] > 0.$$



But  $\lambda_n^- + \lambda_n^+ = \text{tr}(n) = (\beta+1)\mu_n + \gamma \text{tr}(0) > 0$  from (4.11), so that at least  $\lambda_n^+ > 0$ . In order for  $\lambda_n^-$  to be negative, we must have  $\det(n) = \lambda_n^- \lambda_n^+ < 0$ . But  $\det(n) = \gamma^2 T(\frac{\mu_n}{\gamma})$ , so that we are led to make the following assumption on the polynomial  $T$ :

$$(4.24) \quad T(z) \text{ admits 2 positive roots } 0 < z' < z''.$$

Now we have  $\lambda_n^- < 0 \Leftrightarrow z' < \frac{\mu_n}{\gamma} < z'' \Leftrightarrow \frac{\mu_n}{z''} < \gamma < \frac{\mu_n}{z'} \Leftrightarrow \gamma \in I_n = ]z''^{-1}\mu_n, z'^{-1}\mu_n[$ . Thus we have the following result.

Theorem 4.2. Suppose that

- (i)  $\text{tr}(0) = F_s + 1 + F_a + \alpha > 0$
- (ii)  $\det(0) = \alpha F_s + F_a + \alpha > 0$
- (iii)  $\alpha > 1, \beta > 1$
- (iv)  $(\beta(F_s+1) - (F_a+\alpha))^2 + 4\beta F_a F_s > 0$
- (v)  $\beta(F_s+1) + F_a + \alpha < 0$ .

Then there exists a sequence of intervals  $I_n = ]z''^{-1}\mu_n, z'^{-1}\mu_n[$  such that

- (1<sup>0</sup>) if  $\gamma \in \bigcup_{n \geq 1} I_n$  then  $(\tilde{s}, \tilde{a})$  is unstable
- (2<sup>0</sup>) if  $\gamma \in \bigcup_{n \geq 1} I_n$  then  $(\tilde{s}, \tilde{a})$  is stable.

In a similar manner we could define the eigenfunctions

$\psi_n^\pm$  of  $L_\gamma^T$ :

$$(4.25) \quad L_{\gamma}^T \psi_n^{\pm} = \lambda_n^{\pm} \psi_n^{\pm}$$

with the same eigenvalues  $\lambda_n^{\pm}$  but this time, if

$$(4.26) \quad \psi_n^{\pm} = \begin{bmatrix} 1 \\ N_n^{\pm} \end{bmatrix} w_n$$

then  $N_n^{\pm}$  is determined by (in place of (4.21))

$$(4.27) \quad \mu_n + \gamma(F_S + 1) - \lambda_n^{\pm} + \gamma F_a N_n^{\pm} = 0.$$

It can be easily checked that

$$(4.28) \quad \begin{cases} (\phi_n^{\pm}, \psi_n^{\pm}) = 1 + M_n^{\pm} N_n^{\pm} \neq 0 & n \geq 0 \\ (\phi_n^{\pm}, \psi_n^{\mp}) = 0 \\ (\phi_n^{\pm}, \psi_m^{\pm}) = 0 & m \neq n. \end{cases}$$

Here, if  $f = [f_1, f_2]^T \in L^2(\Omega)^2$  and  $g = [g_1, g_2]^T \in L^2(\Omega)^2$ ,  $(f, g)$  means

$$(4.29) \quad (f, g) = \int_{\Omega} (f_1 g_1 + f_2 g_2) d\Omega.$$

Finally, we shall use later the property that the  $\phi_n^{\pm}$  constitute a basis of  $L^2(\Omega)^2$ ; let  $f \in L^2(\Omega)^2$ . Then

$$(4.30) \quad f = \sum_{n \geq 0} f_n^{\pm} \phi_n^{\pm}, \quad (f, \psi_n^{\pm}) = f_n^{\pm} (1 + M_n^{\pm} N_n^{\pm}).$$

Exercise: Prove (4.28).

Hint: From (4.21) and (4.27) we have  $F_a M_n^{\pm} = F_s N_n^{\pm}$  so that

$$1 + M_n^{\pm} N_n^{\pm} = 1 + \gamma^2 M_n^{\pm 2} F_a^2 / \gamma^2 F_s F_a = 1 + (\mu_n + \gamma(F_s + 1) - \lambda_n^{\pm}) / (\beta \mu_n + \gamma(F_a + \alpha) - \lambda_n^{\pm})$$

$$= (\text{tr}(n) - 2\lambda_n^{\pm}) / (\beta \mu_n + \gamma(F_a + \alpha) - \lambda_n^{\pm}) \neq 0.$$

Similarly one can prove the following which will be useful later:

$$1 + \beta M_n^{\pm} N_n^{\pm} = 2\beta\gamma \left( \frac{\mu_n}{\gamma} - \frac{1}{2\beta} (F_a + \alpha + \beta(F_s + 1)) - (\beta + 1)\lambda_n^{\pm} \right) / (\beta \mu_n + \gamma(F_a + \alpha) - \lambda_n^{\pm}).$$

Now  $(\phi_n^{\pm}, \psi_n^{\pm}) = \int_{\Omega} w_n^2 (1 + M_n^{\pm} N_n^{\pm}) d\Omega = 1 + M_n^{\pm} N_n^{\pm}.$

$$(\phi_n^{\pm}, \psi_m^{\pm}) = \left( \int_{\Omega} w_m w_n d\Omega \right) (1 + M_n^{\pm} N_m^{\pm}) = 0 \quad \text{since} \quad \int_{\Omega} w_m w_n d\Omega = \delta_{mn}.$$

Finally,  $\lambda_n^{\pm} (\phi_n^{\pm}, \psi_n^{\pm}) = (L_{\gamma} \phi_n^{\pm}, \psi_n^{\pm}) = (\phi_n^{\pm}, L_{\gamma}^T \psi_n^{\pm}) = \lambda_n^{\pm} (\phi_n^{\pm}, \psi_n^{\pm})$  so that

$$(\phi_n^{\pm}, \psi_n^{\pm}) = 0.$$

In §3 the eigenvalues  $\lambda_n^{\pm}$  and eigenvectors  $\phi_n^{\pm}$  and  $\psi_n^{\pm}$  will be those of  $L_{\gamma_0}$ , where  $\gamma_0$  is a value of the parameter  $\gamma$  for which the trivial steady state  $U = 0$  is losing stability by entering into  $I_{n_0}$ . So that  $\lambda_{n_0}^{\pm} = 0$ ,  $(L_0 + \gamma_0 L_1) \phi_{n_0}^{\pm} = 0$ ,  $(\phi_{n_0}^{\pm}, \psi_{n_0}^{\pm}) = 1 + M_{n_0}^{\pm} N_{n_0}^{\pm} = \text{tr}(n_0) / (\beta \mu_{n_0} + \gamma_0 (F_a + \alpha)) > 0$  and a quantity



which shall be needed later,  $(L_1 \phi_{n_0}^-, \psi_{n_0}^-) = -\frac{1}{\gamma_0} (L_0 \phi_{n_0}^-, \psi_{n_0}^-) =$

$$-\frac{\mu_{n_0}}{\gamma_0} (1 + \beta M_{n_0}^- N_{n_0}^-) = \frac{-\beta \mu_{n_0}}{\beta \mu_{n_0} + \gamma(F_a + \alpha)} \begin{cases} z' - z'' \\ z'' - z' \end{cases} \text{ or } \begin{matrix} \text{or} \\ \text{or} \end{matrix} \text{ according to whether}$$

$$\frac{\mu_{n_0}}{\gamma_0} = z' \text{ or } z''.$$

For similar calculations see Boa's thesis [22].

#### 4.3. Bifurcation analysis

We are going to use the modified perturbation method as indicated in H.B. Keller [23].

Statement of the problem. Let  $\gamma_0$  be a critical value of  $\gamma$ , for which the trivial steady state  $U = 0$  of  $L_\gamma U + M_\gamma(U) = 0$  is losing its stability when  $\gamma$  enters into the interval  $I_{n_0}$ . (i.e.,  $\mu_{n_0}/\gamma_0 = z'$  or  $z''$ , depending upon which extremity of  $I_{n_0}$   $\gamma$  crosses). Let  $\lambda_n^\pm$  be the eigenvalues, and  $\phi_n^\pm$  (resp.  $\psi_n^\pm$ ) be the eigenvectors of  $L_{\gamma_0}$  (resp.  $L_{\gamma_0}^T$ ). We are seeking nontrivial solutions of

$$(4.31) \quad L_\gamma U + \gamma M(U) = 0$$

when  $\gamma$  stays in some neighborhood of  $\gamma_0$ . For that we consider  $U$  and  $\gamma$  as smooth functions of a parameter  $\epsilon$ :

$$(4.32) \quad U = U(\epsilon) \quad \text{and} \quad \gamma = \gamma(\epsilon)$$

satisfying the "inflated" problem

$$(4.33) \quad \begin{cases} (L_0 + \gamma(\epsilon)L_1)U(\epsilon) + \gamma(\epsilon)M(U(\epsilon)) = 0 \\ (U(\epsilon), \psi_{n_0}^-) = \epsilon(1 + M_{n_0}^- N_{n_0}^-) \end{cases}$$

and look for Taylor expansions

$$(4.34) \quad \begin{cases} U(\epsilon) = \epsilon U'(0) + \frac{1}{2}\epsilon^2 U''(0) + o(\epsilon^3) \\ \gamma(\epsilon) = \gamma_0 + \epsilon \gamma'(0) + \frac{1}{2}\epsilon^2 \gamma''(0) + o(\epsilon^3). \end{cases}$$

First, we differentiate equations (4.33) with respect to  $\epsilon$ :

$$(4.35) \quad \begin{cases} \gamma'(\epsilon)L_1 U(\epsilon) + (L_0 + \gamma(\epsilon)L_1)U'(\epsilon) + \gamma'(\epsilon)M(U(\epsilon)) \\ \quad + \gamma(\epsilon)M'(U(\epsilon))U'(\epsilon) = 0 \\ (U'(\epsilon), \psi_{n_0}^-) = 1 + M_{n_0}^- N_{n_0}^- . \end{cases}$$

Then, in (4.35) we put  $\epsilon = 0$

$$(4.36) \quad (L_0 + \gamma_0 L_1)U'(0) = 0, \quad (U'(0), \psi_{n_0}^-) = 1 + M_{n_0}^- N_{n_0}^-$$

since  $U(0) = 0$ ,  $M(0) = 0$  and  $M'(0) = 0$ .

From (4.36) it results that

$$(4.37) \quad U'(0) = \phi_{n_0}^-$$

Now we differentiate equations (4.35) with respect to  $\epsilon$ , and omit  $\epsilon$  everywhere to simplify notation:

$$(4.38) \quad \begin{cases} \gamma'' L_1 U + 2\gamma' L_1 U' + (L_0 + \gamma L_1) U'' + \gamma'' M(U) + 2\gamma' M'(U) U' \\ \quad + \gamma M''(U) U'^2 + \gamma M'(U) U'' = 0 \\ (U'', \psi_{n_0}^-) = 0. \end{cases}$$

In (4.38) we again put  $\epsilon = 0$ :

$$(4.39) \quad \begin{cases} 2\gamma'(0) L_1 \phi_{n_0}^- + (L_0 + \gamma_0 L_1) U''(0) + \gamma_0 M''(0) \phi_{n_0}^{-2} = 0, \\ (U''(0), \psi_{n_0}^-) = 0. \end{cases}$$

From the Fredholm alternative, (4.39) will have a solution for  $U''(0)$  if and only if

$$(4.40) \quad (2\gamma'(0) L_1 \phi_{n_0}^- + \gamma_0 M''(0) \phi_{n_0}^{-2}, \psi_{n_0}^-) = 0.$$



This relation gives  $\gamma'(0)$ :

$$(4.41) \quad \gamma'(0) = -\gamma_0 \frac{(M''(0) \phi_{n_0}^{-2}, \psi_{n_0}^-)}{2(L_1 \phi_{n_0}^-, \psi_{n_0}^-)}.$$

Recall that at the end of §2 we did calculate the denominator of (4.41). On the other hand the numerator must be interpreted in the following way:

$$M(U) = N(U) \begin{bmatrix} 1 \\ 1 \end{bmatrix} = (F(\tilde{s}+u, \tilde{a}+v) - F(\tilde{s}, \tilde{a}) - F_s u - F_a v) \begin{bmatrix} 1 \\ 1 \end{bmatrix}.$$

$$\text{If } H = [h_1, h_2]^T,$$

$$(M'(U), H) = (F'_s(\tilde{s}+u, \tilde{a}+v)h_1 + F'_a(\tilde{s}+u, \tilde{a}+v)h_2 - F_s h_1 - F_a h_2) \begin{bmatrix} 1 \\ 1 \end{bmatrix}$$

$$M''(U)(H, K) = (F''_{ss}(\tilde{s}+u, \tilde{a}+v)h_1 k_1 + F''_{sa}(\tilde{s}+u, \tilde{a}+v)(h_1 k_2 + h_2 k_1) + F''_{aa}(\tilde{s}+u, \tilde{a}+v)h_2 k_2) \begin{bmatrix} 1 \\ 1 \end{bmatrix}$$

$$M'''(U)(H, K, L) = (F'''_{sss} h_1 k_1 \ell_1 + F'''_{ssa} (h_1 k_1 \ell_2 + h_1 k_s \ell_1 + h_2 k_1 \ell_1) + F'''_{saa} (h_1 k_2 \ell_2 + h_2 k_1 \ell_2 + h_2 k_2 \ell_1) + F'''_{aaa} h_2 k_2 \ell_2) \begin{bmatrix} 1 \\ 1 \end{bmatrix}.$$

From this, and the fact that  $F''_{aa} = 0$ , we find

$$(4.42) \quad (M''(0)\phi_{n_0}^{-2}, \psi_{n_0}^{-}) = (F_{ss}'' + 2F_{sa}'' M_{n_0}^{-})(1 + N_{n_0}^{-}) \left( \int_{\Omega} w_{n_0}^3 d\Omega \right).$$

In the case where  $\int_{\Omega} w_{n_0}^3 d\Omega = 0$  we have

$$(4.43) \quad \gamma'(0) = 0$$

and the bifurcation will be unilateral (Figure 4.4 (a), (b)). Otherwise, (this will be the general case) the bifurcation will be 2 sided (Figure 4.4 (c), (d)).

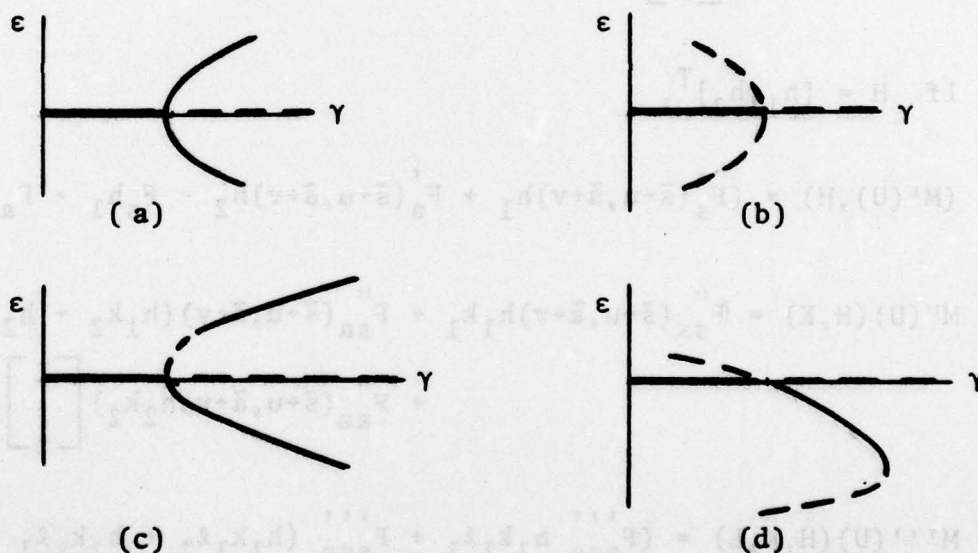


Figure 4.4

So the only case where one needs further information is the case where (4.43) holds. In that case we would like to know on what

side of  $\gamma_0$  the bifurcated branch lies, i.e., know  $\gamma''(0)$ .

When (4.40) holds  $U''(0)$  is given explicitly by

$$(4.44) \quad U''(0) = -\gamma_0 \sum_{\lambda_n^{\pm} \neq 0} \frac{1}{\lambda_n^{\pm}} (M''(0) \phi_{n_0}^{-2}, \psi_n^{\pm}) \frac{1}{1+M_n^{\pm} N_n^{\pm}} \phi_n^{\pm}.$$

Now in order to get  $U''(0)$  we differentiate once more in (4.38)

and set  $\varepsilon = 0$  (recall that  $\gamma'(0) = 0$ ):

$$3\gamma''(0)L_1\phi_{n_0}^{-} + (L_0 + \gamma_0 L_1)U'''(0) + \gamma_0 M'''(0)\phi_{n_0}^{-3} + 3\gamma_0 M''(0)\phi_{n_0}^{-} U''(0) = 0.$$

The condition for existence of  $U'''(0)$  is

$$(4.45) \quad \gamma''(0) = - \frac{\gamma_0}{3(L_1\phi_{n_0}^{-}, \psi_{n_0}^{-})} ((M'''(0)\phi_{n_0}^{-3}, \psi_{n_0}^{-}) + 3(M''(0)\phi_{n_0}^{-} U''(0), \psi_{n_0}^{-}))$$

and this quantity can be calculated.

**Remark.** In the case of a 2- or 3- dimensional domain  $\Omega$  with arbitrary shape, there is no reason for (4.43) to hold. However, in the 1-dimensional case, where  $w_n(x) = \cos n\pi x$ ,  $\int_0^1 w^3 dx = 0$ .

Also when  $\Omega$  has 1 axis of symmetry, say 0 -  $y$  suppose that  $w$  is an eigenfunction:

$$-\Delta w(x,y) = \lambda w(x,y) \quad , \quad \int_{\Omega} w^2 d\Omega = 1$$



and consider  $v(x,y) = w(-x,y)$ .

$$-\Delta v(x,y) = -\Delta w(-x,y) = \lambda w(-x,y) = \lambda v(x,y), \quad \int_{\Omega} v^2 d\Omega = 1$$

Then  $v(x,y) = \pm w(x,y)$ , i.e.,  $w(-x,y) = \pm w(x,y)$ , so that there is the possibility for  $w$  to satisfy  $w(-x,y) = -w(x,y)$ . In that case  $\int_{\Omega} w^3 d\Omega = 0$  and (4.43) holds.

The case  $\Omega = ]0,1[$  is not unrealistic. It corresponds to the modelling of an ellipsoid with large axis ratio when one is interested in the first eigenmodes. One can explain the differentiation of regions in an egg by a steady pattern as pictured in Figure 4.5 (Kauffman et al [18]). See also §5.

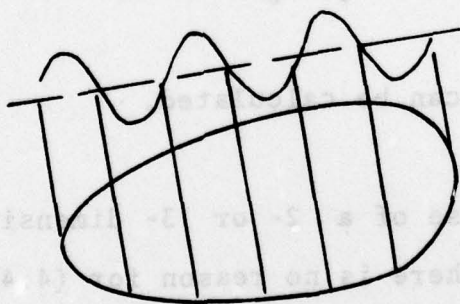


Figure 4.5

#### 4.4. Numerical analysis.

Two kinds of methods are at our disposal:

- (i) methods in which the steady states are obtained by solving the evolution equations until one estimates that the system has attained a (stable) steady state; and
- (ii) methods following branches of (stable or unstable) steady state solutions.

The second type of method was discussed in Chapter 2.

#### Solution of the evolution equations.

##### (a) Discretization with respect to time:

$$(4.46) \quad \begin{cases} \frac{s^{n+1} - s^n}{\Delta t} - \Delta s^{n+1} + \gamma[F(s^n, a^n) - (s_0 - s^{n+1})] = 0 \\ \frac{a^{n+1} - a^n}{\Delta t} - \beta \Delta a^{n+1} + \gamma[F(s^n, a^n) - \alpha(a_0 - a^{n+1})] = 0. \end{cases}$$

##### (b) Discretization with respect to space:

By finite differences in the 1-dimensional case, (by finite elements in the 2-dimensional case (Figure 4.6)) (4.46) can be written

$$(4.47) \quad \begin{cases} (K + (\frac{1}{\Delta t} + \gamma)M)S^{n+1} = Mf^n \\ (\beta K + (\frac{1}{\Delta t} + \gamma\alpha)M)A^{n+1} = Mg^n, \end{cases}$$

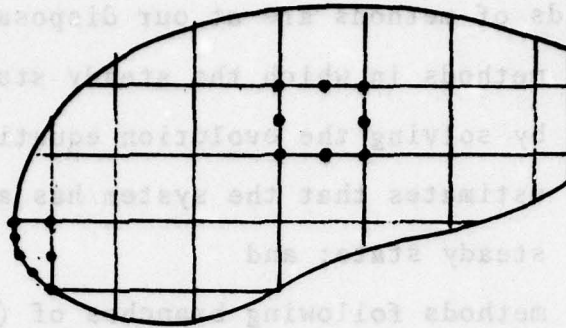


Figure 4.6

where

$K$  = stiffness matrix (corresponding to  $-\Delta$ )

$M$  = mass matrix (corresponding to  $I$ )

$f^n$  = vector  $\frac{s^n}{\Delta t} - \gamma(F(s^n, a^n) - s_0)$

$g^n = \frac{a^n}{\Delta t} - \gamma(F(s^n, a^n) - \alpha a_0).$

For the practical formulation and implementation of the finite element method we refer to Bathe and Wilson [15]. Let us give more details on the calculation of the "stiffness" and "mass" matrices  $K$  and  $M$  in the case of a surface (a planar domain being a particular case). The surface is divided into curved 8-nodes quadrilaterals (see Figure 4.7). The nodes are defined by their coordinates  $(x_i, y_i, z_i)$  for node number  $i$  of the quadrilateral,  $1 \leq i \leq 8$ ). We call  $H_i(r, s)$  the "shape functions":



$$\begin{cases}
 H_1(r,s) = \frac{1}{4}(1+r)(1+s) - \frac{1}{2}H_5(r,s) - \frac{1}{2}H_8(r,s) \\
 H_2(r,s) = \frac{1}{4}(1-r)(1+s) - \frac{1}{2}H_6(r,s) - \frac{1}{2}H_5(r,s) \\
 H_3(r,s) = \frac{1}{4}(1-r)(1-s) - \frac{1}{2}H_7(r,s) - \frac{1}{2}H_6(r,s) \\
 H_4(r,s) = \frac{1}{4}(1+r)(1-s) - \frac{1}{2}H_8(r,s) - \frac{1}{2}H_7(r,s) \\
 H_5(r,s) = \frac{1}{2}(1-r^2)(1+s) \\
 H_6(r,s) = \frac{1}{2}(1-s^2)(1-r) \\
 H_7(r,s) = \frac{1}{2}(1-r^2)(1-s) \\
 H_8(r,s) = \frac{1}{2}(1-s^2)(1+r).
 \end{cases}$$

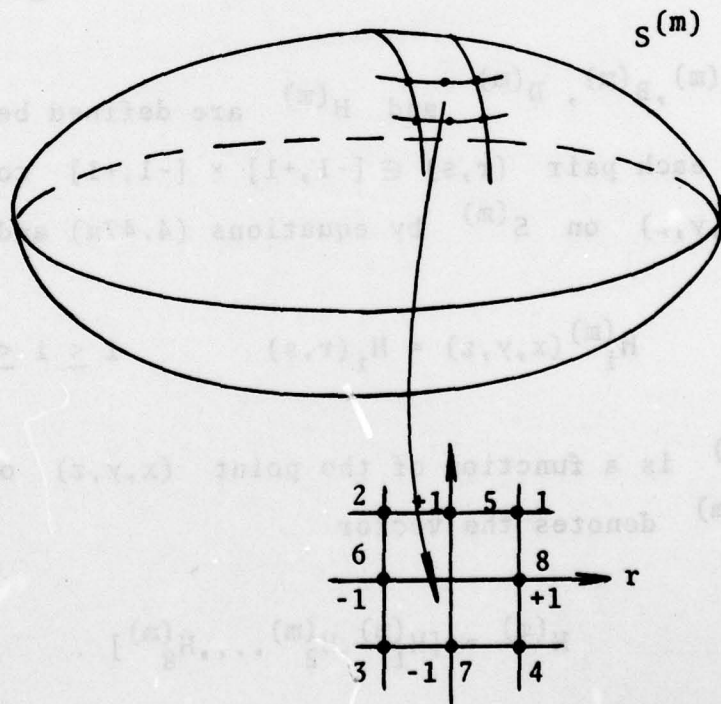


Figure 4.7

The part of the surface delineated by the quadrilateral is approximated by the surface  $S^{(m)}$  whose parametric representation is

$$(4.47a) \quad \begin{cases} x = \sum_{i=1}^8 x_i H_i(r,s), & y = \sum_{i=1}^8 y_i H_i(r,s), & z = \sum_{i=1}^8 z_i H_i(r,s) \\ -1 \leq r, s \leq +1. \end{cases}$$

The elementary mass and stiffness matrices are

$$K^{(m)} = \int_{S^{(m)}} B^{(m)T} D^{(m)} B^{(m)} dS^{(m)} \quad \text{and} \quad M^{(m)} = \int_{S^{(m)}} H^{(m)T} H^{(m)} dS^{(m)}$$

where  $dS^{(m)}$ ,  $B^{(m)}$ ,  $D^{(m)}$  and  $H^{(m)}$  are defined below.

To each pair  $(r,s) \in [-1,+1] \times [-1,+1]$  corresponds a point  $(x,y,z)$  on  $S^{(m)}$  by equations (4.47a) and we call

$$H_i^{(m)}(x,y,z) = H_i(r,s) \quad 1 \leq i \leq 8.$$

Thus  $H_i^{(m)}$  is a function of the point  $(x,y,z)$  on the surface  $S^{(m)}$ .  $H^{(m)}$  denotes the vector

$$H^{(m)} = [H_1^{(m)}, H_2^{(m)}, \dots, H_8^{(m)}] .$$

Similarly we define

$$B^{(m)} = \begin{bmatrix} \frac{\partial H_1}{\partial r} & \dots & \frac{\partial H_8}{\partial r} \\ \frac{\partial H_1}{\partial s} & \dots & \frac{\partial H_8}{\partial s} \end{bmatrix}.$$

$H^{(m)}$  and  $B^{(m)}$  are  $8 \times 1$  and  $8 \times 2$  matrices defined on  $S^{(m)}$ .

Now, following equations (1.33)-(1.36) of Chapter I, we define

$$\begin{aligned} dl^2 &= dx^2 + dy^2 + dz^2 = \left( \sum_{i=1}^8 x_i \frac{\partial H_i}{\partial r} dr + \frac{\partial H_i}{\partial s} ds \right)^2 \\ &\quad + \left( \sum y_i \left( \frac{\partial H_i}{\partial r} dr + \frac{\partial H_i}{\partial s} ds \right) \right)^2 + \left( \sum z_i \left( \frac{\partial H_i}{\partial r} dr + \frac{\partial H_i}{\partial s} ds \right) \right)^2 \\ &= a_{11} dr^2 + 2a_{12} dr ds + a_{22} ds^2 \\ a_{11} &= \vec{V}_1^2, \quad a_{12} = \vec{V}_1 \vec{V}_2, \quad a_{22} = \vec{V}_2^2 \\ \vec{V}_1 &= \left[ \sum_{i=1}^8 x_i \frac{\partial H_i}{\partial r}, \sum y_i \frac{\partial H_i}{\partial r}, \sum z_i \frac{\partial H_i}{\partial r} \right]^T \\ \vec{V}_2 &= \left[ \sum x_i \frac{\partial H_i}{\partial s}, \sum y_i \frac{\partial H_i}{\partial s}, \sum z_i \frac{\partial H_i}{\partial s} \right]^T. \end{aligned}$$

Then we define

$$a = a_{11}a_{22} - a_{12}^2$$

$$a^{11} = a_{22}/a, \quad a^{22} = a_{11}/a, \quad a^{12} = -a_{12}/a$$



$$dS^{(m)} = a^{1/2} dr ds,$$

$$D^{(m)} = \begin{bmatrix} a^{11} & a^{12} \\ a^{12} & a^{22} \end{bmatrix},$$

$$K^{(m)} = \int_{-1 \leq r, s \leq +1} B^{(m)T} D^{(m)} B^{(m)} a^{1/2} dr ds,$$

$$M^{(m)} = \int_{-1 \leq r, s \leq +1} H^{(m)T} H^{(m)} a^{1/2} dr ds.$$

Using this method and the program SSPACE (subspace iteration method) of Bathe and Wilson [15], the first eigenvalues and eigenfunctions of the Laplace Beltrami operator  $-\Delta_B$  on the surface of an elongated ellipsoid with the form of an egg can be obtained (Bunow et.al. [24]), (See Figures 4.8, 4.9).

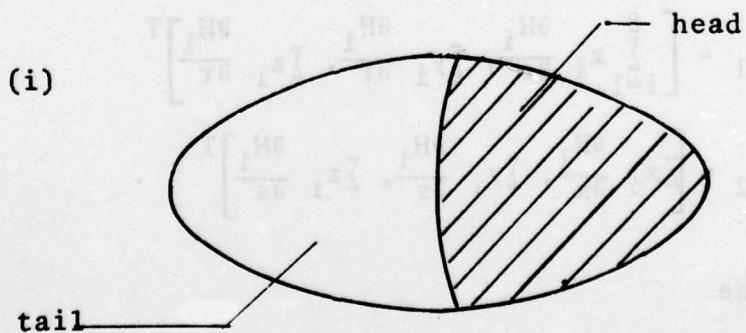


Figure 4.8

AD-A078 591

BROWN UNIV PROVIDENCE R I LEFSCHETZ CENTER FOR DYNAM--ETC F/G 6/1  
MATHEMATICAL ANALYSIS OF ARTIFICIAL ENZYMATICALLY ACTIVE MEMBRA--ETC(U)  
MAY 79 J P KERNEVEZ  
LCDS-LN-79-2

UNCLASSIFIED

ARO-13915.27-M

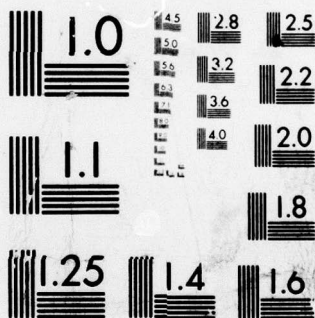
NL

2 OF 2

AD  
A078591



END  
DATE  
FILMED  
1-80  
DDC



MICROCOPY RESOLUTION TEST CHART  
NATIONAL BUREAU OF STANDARDS-1963-A



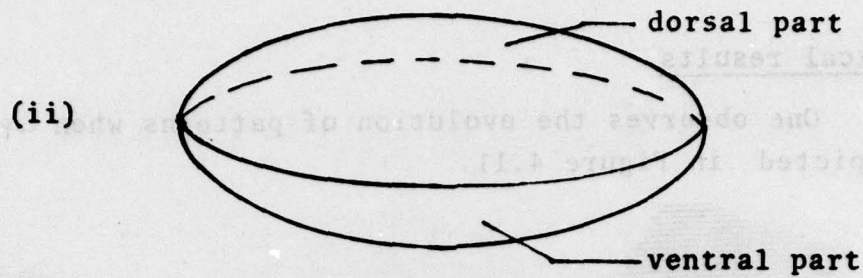
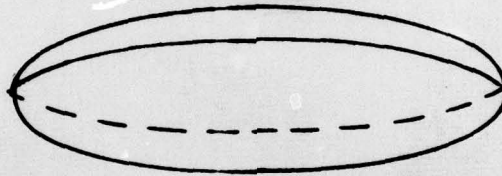


Figure 4.9

(iii) separation between left and right sides  
etc...



Surfaces where the diffusion coefficients are varying (because of a layer of cells of variable size for instance) model more closely the shape of the real imaginal discs (Figure 4.10). It is thus possible to solve the S-A system equations on such surfaces and study the sequence of stable patterns.

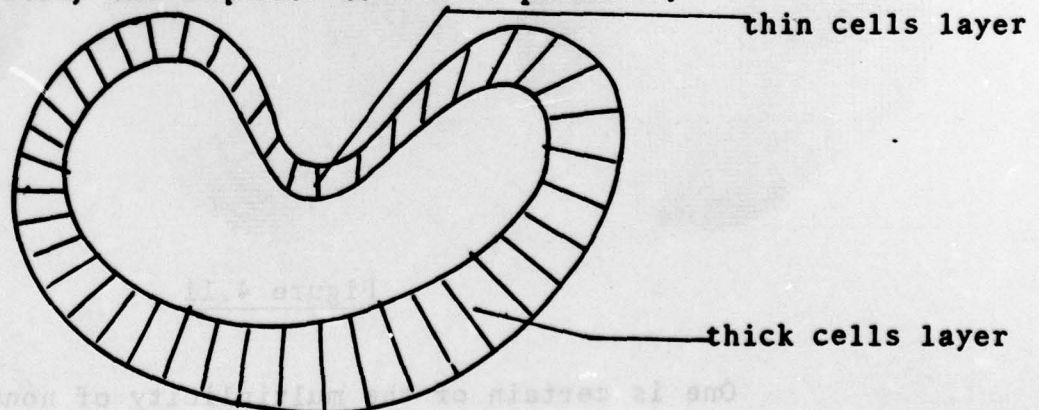


Figure 4.10

Section of an imaginal disc

### Numerical results

One observes the evolution of patterns when  $\gamma$  varies as depicted in Figure 4.11.

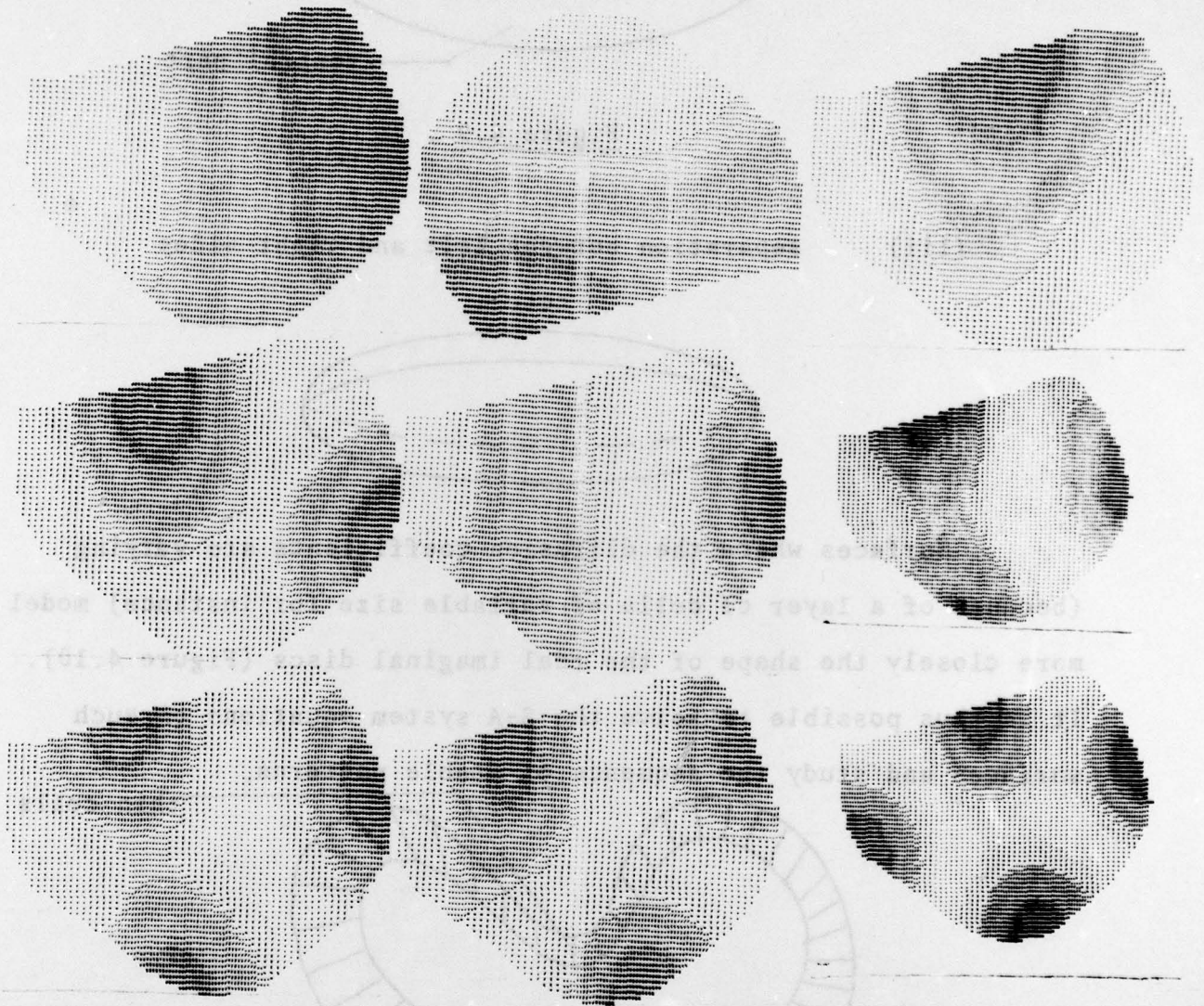
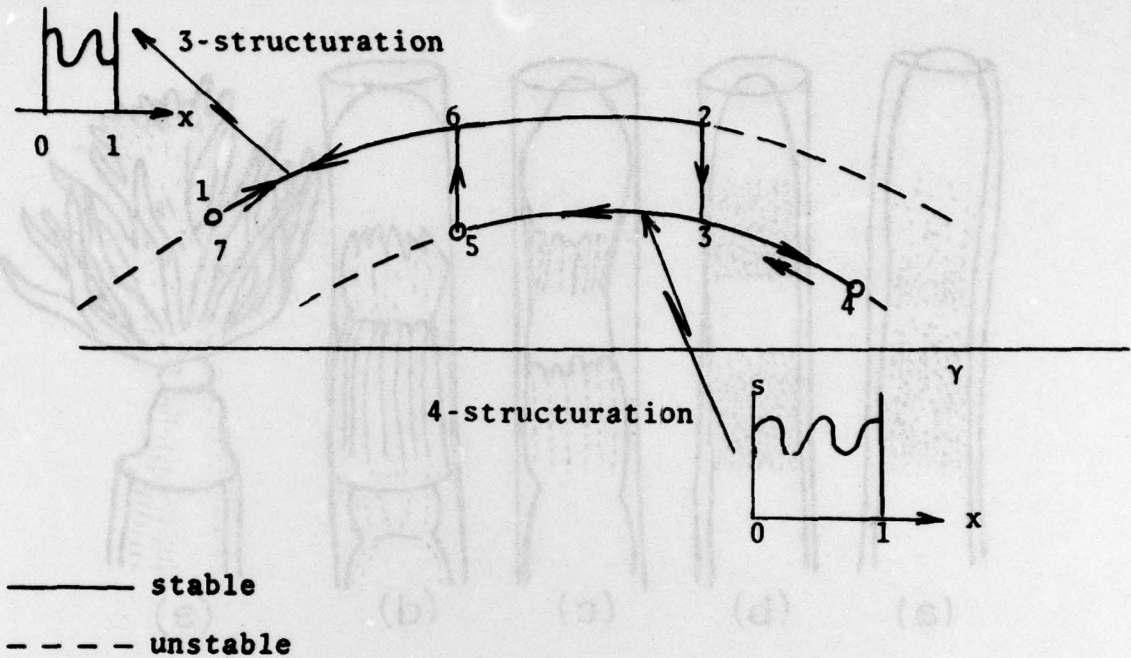


Figure 4.11

One is certain of the multiplicity of nonuniform steady-



states (N.U.S.S.) from the numerical results in the 1-dimensional case, where one has situations as in Figure 4.12.



**Figure 4.12**

Hysteresis cycle when  $\gamma$  first increases, then decreases, the steady state following the path 1-2-3-4-5-6-7.



#### 4.5. Hydranth regeneration in Tubularia

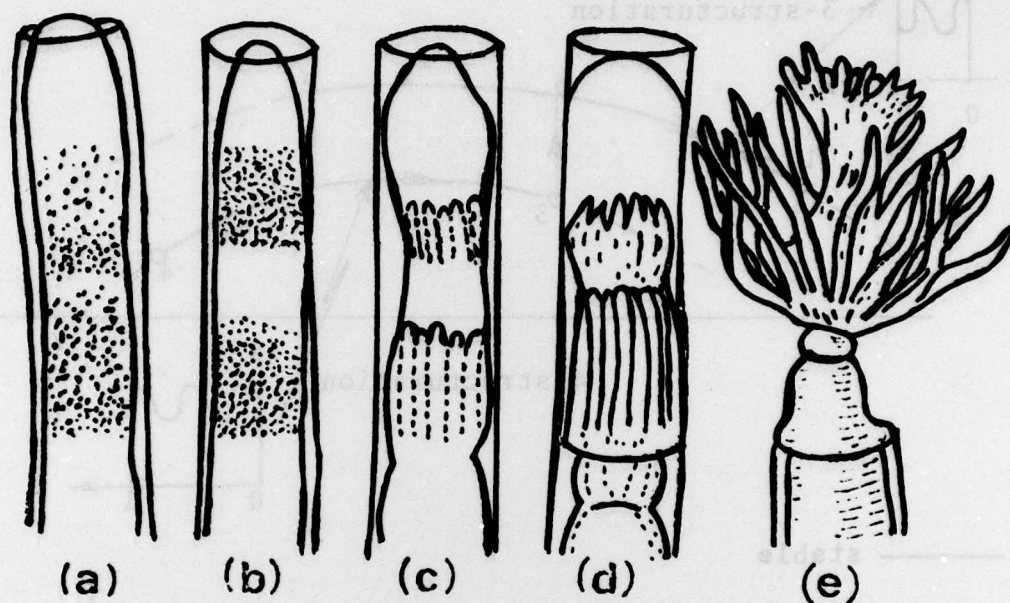


Figure 4.13

Reaction - diffusion model of Murray et al [25], for the hydranth regeneration in the marine hydroid *Tubularia*.

Pigment distribution presages hydranth regeneration of an amputated hydranth in the marine hydroid *Tubularia*. Murray, et al, [25], suggest that such a distribution could result from a reaction diffusion system. In the marine hydroid *Tubularia* regeneration of an amputated hydranth takes place in the order of one and a half days. The sequence of clearly observable states is illustrated

schematically in Figure 4.13. In Figure 4.13 (a), (b) and (c) the shading and serrated lines represent clearly seen reddish coloured pigment. The regular periodic configuration in Figure 4.13(c) presages the tentacle distribution in Figure 4.13 (d). Murray considers the body of the Tubularia to be represented by a circular cylinder of internal radius  $r_1$  and external radius  $r_2$  and considers the reaction-diffusion mechanism model to be similar to the  $s - a$  system with  $\alpha = 1.5$ ,  $\beta = 100$ ,  $k = 0.1$ ,  $s_0 = 92$ ,  $a_0 = 65$ ,  $\rho = 18.5$  ( $\tilde{s} = 10$ ,  $\tilde{a} = 9.4$ ) and various  $\gamma$ . Either  $s$  or  $a$  is related to the pigmentation and their spatial structure indicates the colouration.

The axial distribution in Figure 4.13 (a) and (b) is explained by the 1-dimensional version of the  $s - a$  system.

The circumferential distribution in Figure 4.13 (c) can be produced by a 2-dimensional version of the  $s - a$  system in the geometry obtained by a cross section of the finite wall cylinder.

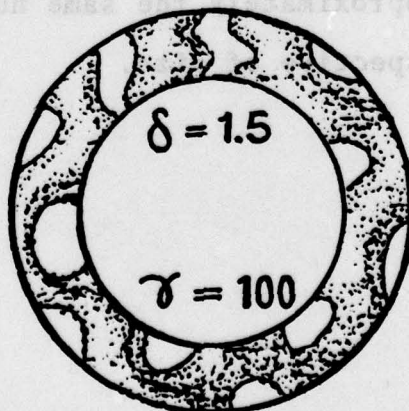


Figure 4.14

patterns in a cross section of the finite wall cylinder



The typical length  $L$  is  $r_1$ . The reaction-diffusion domain is then given by  $1 < r < \delta$  ( $\delta = r_2/r_1$ ) and the equations are

$$(4.48) \quad \begin{cases} \frac{\partial s}{\partial t} - \left( \frac{\partial^2 s}{\partial r^2} + \frac{1}{r} \frac{\partial s}{\partial r} + \frac{1}{r^2} \frac{\partial^2 s}{\partial \theta^2} \right) + \gamma f(s, a) = 0 \\ \frac{\partial a}{\partial t} - \beta \left( \frac{\partial^2 a}{\partial r^2} + \frac{1}{r} \frac{\partial a}{\partial r} + \frac{1}{r^2} \frac{\partial^2 a}{\partial \theta^2} \right) + \gamma g(s, a) = 0 \end{cases}$$

with the boundary conditions

$$(4.49) \quad \frac{\partial s}{\partial r} = \frac{\partial a}{\partial r} = 0 \quad \text{for } r = 1, r = \delta.$$

Murray notes that the number of tentacles is independent of overall size, if, all other parameters being constant, the ratio  $\frac{r_2}{r_1} = \delta$  is kept fixed. This could explain the regulating feature of *Tubularia* that approximately the same number of tentacles appear, roughly 12-18, irrespective of size.



## REFERENCES

- [1] R. Aris, The Mathematical Theory of Diffusion and Reaction in Permeable Catalysts, Vol. I and II, Clarendon Press, Oxford, 1975.
- [2] G. Nicolis and I. Prigogine, Self-organization in non-equilibrium systems, Wiley Interscience, 1977.
- [3] J. D. Murray, Lectures on Nonlinear-Differential-Equation Models in Biology, Clarendon Press, Oxford, 1977.
- [4] P. C. Fife, Mathematical Aspects of Reacting and Diffusing Systems, Lecture Notes in Biomathematics 28, Springer-Verlag, Berlin, 1979.
- [5] L. Michaelis and M. I. Menten, Die Kinetik der Invertinwirkung, Biochem. Z., 49 (1913), pp. 333-369.
- [6] M. Dixon and E. C. Webb, Enzymes, Academic Press, New York, 1964.
- [7] H. T. Banks, Modeling and Control in the Biomedical Sciences, Lecture Notes in Biomathematics 6, Springer-Verlag, Berlin, 1975.
- [8] D. Thomas and G. Broun, Artificial enzyme membranes, Methods in Enzymology, 44(1976), pp. 901-929.
- [9] D. Thomas, Production of biological catalysts, stabilization and exploitation: "necessity, content and management principles of a possible community action in Biotechnology", ECSC-EEC-EAEC, Brussels-Luxembourg, 1978.
- [10] J. P. Kernevez and D. Thomas, Numerical analysis and control of some biochemical systems, Applied Math. & Optimization, 1(1975), pp.222-285.
- [11] B. Bunow and C. Colton, Substrate inhibition kinetics in assemblages of cells, Biosystems, 5(1975).
- [12] C. M. Brauner and B. Nicolaenko, Singular perturbation, multiple solutions and hysteresis in a nonlinear problem, Lecture Notes in Math. #594, Springer-Verlag, Berlin, 1977, pp.50-76.

- [13] C. M. Brauner and B. Nicolaenko, Sur une classe de problèmes elliptiques nonlinéaires, CRAS, t-286, Série A, (1978), pp.1007-1010.
- [14] M. Kubicek, Algorithm 502, Dependence of solution of non-linear systems on a parameter, ACM Transactions on Math. Software, 2(1), (1976), pp.98-107.
- [15] K. Bathe and E. Wilson, Numerical Methods in Finite Element Analysis, Prentice Hall, Englewood Cliffs, N.J., 1976.
- [16] F. Murat et J. Simon, Quelques résultats sur le contrôle par un domaine géométrique, Université Paris VI #74003, (1976).
- [17] F. Mignot, F. Murat, J. P. Puel, Variation d'un point de retournement par rapport au domaine Université Paris VI, (1978).
- [18] S. A. Kauffman, R. M. Shymko and K. Trabert, Control of sequential compartment formation, Drosophila Science, 199(1978), pp.259-270.
- [19] A. M. Turing, The chemical basis of morphogenesis, Phil. Trans. Roy. Soc. Vol. B237, (1952), pp.37-72.
- [20] J. P. Kernevez, G. Joly, M. C. Duban, B. Bunow and D. Thomas, Hysteresis, oscillations, and pattern formation in realistic immobilized enzyme systems, J. Math. Biology 7, (1979), pp.41-56.
- [21] J. P. Kernevez, G. Joly, D. Thomas and B. Bunow, Pattern formation and wave propagation in the s - a system, Lecture Notes in Math, Proceedings, Conf. on Non-linear Eigen Problems, Villetaneuse.
- [22] J. Bo, A Model Biochemical Reaction, Ph.D. thesis, Calif. Inst. Tech., Pasadena, Calif. 1974.
- [23] H. B. Keller, Lecture notes on perturbation theory, Math. Dept., Michigan State University, March, 1968.
- [24] B. Bunow and J. P. Kernevez, A finite element approximation of the Laplace Beltrami operator on a surface.  
Submitted



- [25] J. D. Murray, N. F. Britton, G. Joly and M. C. Duban,  
A model for hydranth regeneration in Tubularia. To appear.
- [26] G. Meurant and J.C. Saut, Bifurcation and stability in a  
classical system, J. Math. Anal. and Appl. 50(1977), pp.69-91.
- [27] M. C. Duban, Hystérésis, oscillations et structurations en  
espace dans des systemes biochimiques distribués,  
Thèse, U.T.C., March, 1977.
- [28] C. A. Felippa, Solution of linear equations with skyline  
stored symmetric matrix, Comput. Structures 5(1975),  
pp.13-29.
- [29] G. Joly, Identification de Paramètres Cinétiques dans des  
Systèmes Biochimiques, Thesis, 1974, Paris.
- [30] H. Ashkenazi and H.G. Othmer, Spatial patterns in coupled  
biochemical oscillators, J. Math. Biology 5(1978),  
pp.305-350.